



Characterization of initial events of bacterial colonization at solid-water interfaces using image analysis
by Robert Franz Mueller

A thesis submitted in partial fulfillment of the requirements for the degree of Master of Science in
Environmental Engineering
Montana State University
© Copyright by Robert Franz Mueller (1990)

Abstract:

The processes leading to bacterial accumulation on solid-water interfaces are adsorption, desorption, growth, and erosion. These processes have been measured individually in-situ in a flowing system and in real time using image analysis. The flow was laminar ($Re = 1.4$) and the shear stress was kept constant during all experiments at 0.75 Nm^{-2} . Five different substrata -- copper, silicon, 316 stainless steel, glass, and polycarbonate -- and three different bacterial strains -- *Pseudomonas aeruginosa*, *Pseudomonas fluorescens* (mot+) and *Pseudomonas fluorescens* (mot-) -- were used in the experiments. The surface roughness varied among the substrata from 25 Å for silicon as the smoothest substratum to 150 Å for copper as the roughest substratum. The effects of nutrient limitation and starvation of cells on sorption phenomena were also examined.

Sorption related processes were found to be influenced by the surface properties of the substrata and by the nature of the bacterial strain. Adsorption velocity was positively correlated with the surface roughness of the substratum and the surface hydrophobicity of the cells. While the sticking efficiency of a non-motile strain was found to be much higher than the corresponding motile strain, the motile cells adsorbed more rapidly due to superior transport properties arising from motility. Starvation of *Pseudomonas aeruginosa* cells was observed to result in a lower sticking efficiency, but increased motility resulting from dwarfing/fragmentation of the cells. Copper was found to inhibit cell growth on its surface, but the metal oxide layer on the surface as well as an already formed biofilm protected the cells and replication was observed after a longer exposure time to cell-containing bulk water. A mathematical model was developed to predict cell accumulation on a substratum, based on kinetic data for adsorption, desorption, growth, and erosion, for each of the tested substrata and organisms.

CHARACTERIZATION OF INITIAL EVENTS OF BACTERIAL COLONIZATION

AT SOLID-WATER INTERFACES USING IMAGE ANALYSIS

by

Robert Franz Mueller

A thesis submitted in partial fulfillment
of the requirements for the degree

of

Master of Science

in

Environmental Engineering

MONTANA STATE UNIVERSITY
Bozeman, Montana

June 1990

N378
M8869

APPROVAL

of a thesis submitted by

Robert Franz Mueller

This thesis has been read by each member of the thesis committee and has been found to be satisfactory regarding content, English usage, format, citations, bibliographic style, and consistency, and is ready for submission to the College of Graduate Studies.

6/18/90
Date

W. Haralick 6/18/90
Chairperson, Graduate Committee

Approved for the Major Department

18 June '90
Date

Shedue E. Lang
Head, Major Department

Approved for the College of Graduate Studies

June 18, 1990
Date

Henry L. Parsons
Graduate Dean

STATEMENT OF PERMISSION TO USE

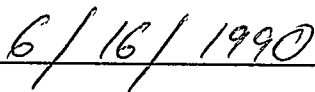
In presenting this thesis in partial fulfillment of the requirements for a master's degree at Montana State University, I agree that the Library shall make it available to borrowers under rules of the Library. Brief quotations from this thesis are allowable without special permission, provided that accurate acknowledgement of source is made.

Permission for extensive quotation from or reproduction of this thesis may be granted by my major professor, or in his absence, by the Dean of Libraries when, in the opinion of either, the proposed use of material is for scholarly purposes. Any copying or use of the material in this thesis for financial gain shall not be allowed without my written permission.

Signature



Date



ACKNOWLEDGEMENTS

I would like to thank all IPA/ERC members for providing an enjoyable environment and helping me with this study. I especially would like to thank Bill Characklis for his advice and guidance, Warren Jones and Ann Camper for their help and numerous discussions, John Sears for making this study possible, Kay Smith for her help, and Gordon Williams, John Rompel, and Paul Stoodley are thanked for their technical and analytical support, also. Diane, Linda, Wendy, and Jamie provided assistance and moral support during my stay in Bozeman.

In particular I would like to express my appreciation to John Stover, Roger Colberg, and Marvin Bernt at TMA Technologies, Inc. Bozeman who helped me with their light scatter measurements and Doug Caldwell from Vancouver, British Columbia for contributing his Pseudomonas fluorescens.

Last not least I would like to thank my Bozeman climbing friends who gave me joy, challenge, and a good escape from the laboratory who never tired of playing on those "stones" with me.

TABLE OF CONTENTS

	Page
LIST OF TABLES	viii
LIST OF FIGURES	ix
ABSTRACT	xi
INTRODUCTION	1
Goal of Research	3
Objectives of Research	3
BACKGROUND	4
Overview	4
Previous Research	4
Surface Free Energy	5
Surface Roughness	6
Hydrodynamic Factors	7
Chemical Factors	7
Microbiological Factors	8
Nutrient Availability - Starvation	8
THEORY	10
Process Analysis at the Solid-Liquid Interface	10
Rate Coefficients of	
Early Surface Colonization	12
Growth on Surfaces	13
Cell Balance at the Substratum-	
Bulk Water Interface	14
Process Analysis for Chemostat Operation	15
Modified Chemostat Operation for Starvation	16
Transport	18
Diffusivity of Motile Cells	18
Diffusivity of Non-Motile Cells	19
Transport to the Solid-Liquid Interface	20
Adsorption Velocity	22
Sticking Efficiency	23
Fluid Dynamics	24
Reynolds Number	25
METHODS	26
Experimental System	26
Method of Analysis	29
Total Cell Counts	29
Viable Cell Counts	29
Cell Surface Hydrophobicity	29
Total Organic Carbon	30
Dissolved Organic Carbon	30
Surface Roughness	31

TABLE OF CONTENTS (Continued)

	Page
Estimation of Cell Motility	31
Determination of Rate of Adsorption and Desorption on the Substratum	32
Determination of the Rate of Growth and Erosion on the Substratum	32
Image Analysis	33
RESULTS	34
Chemostat Operation	34
Image Processing	35
Cell Surface Hydrophobicity	35
<u>Pseudomonas aeruginosa</u> , Kinetic Results	36
Surface Colonization of <u>Pseudomonas aeruginosa</u>	36
Copper	36
Silicon	39
316 Stainless Steel	41
Surface roughness	43
<u>Pseudomonas fluorescens</u> (mot+), Results	43
Surface Colonization of	
<u>Pseudomonas fluorescens</u> (mot+)	43
316 Stainless Steel	44
Polycarbonate	45
Glass	45
Surface Roughness	47
Results with <u>Pseudomonas fluorescens</u> (mot-)	47
Surface Colonization of	
<u>Pseudomonas fluorescens</u> (mot+)	47
316 Stainless Steel	48
Polycarbonate	48
Glass	48
Surface Colonization and Dislocations on Stainless Steel	50
<u>Pseudomonas aeruginosa</u> , Starvation and Adsorption to 316 Stainless Steel	51
Dwarfing and Fragmentation	52
Surface Colonization of Starved	
<u>Pseudomonas aeruginosa</u> on 316 Stainless Steel	54
Cellular Motility	54
SIMULATION OF CELL ACCUMULATION	57
Bulk Water Cell Concentration	57
Fluid Shear Stress	57
Substrata and Bulk Water Nutrient Concentration	58
Mixed Populations	58

TABLE OF CONTENTS (Continued)

	Page
DISCUSSION	62
Comparison of <u>Pseudomonas</u>	
<u>aeruginosa</u> on Various Substrata	62
Comparison of <u>Pseudomonas aeruginosa</u>	
and <u>Pseudomonas fluorescens</u> (mot+)	67
Comparison of Mot+ and Mot- <u>Pseudomonas fluorescens</u>	70
Influence of Starvation on Colonization of	
<u>Pseudomonas aeruginosa</u> on 316 Stainless Steel	72
CONCLUSIONS	75
NOMENCLATURE/SYMBOLS	77
Nomenclature	78
Symbols	79
LITERATURE CITED	81
APPENDIX	86
Cell Accumulation at Various	
Durations of Starvation	87

LIST OF TABLES

Table	Page
1. Chemical Composition of Nutrient	27
2. System Specific Parameters	27
3. Cell surface Hydrophobicity	35
4. <u>Pseudomonas aeruginosa</u> , Summary of the Results	43
5. <u>Pseudomonas flouescens</u> (mot+), Summary of the Results	47
6. <u>Pseudomonas flouescens</u> (mot-), Summary of the Results	50
7. Starvation of <u>Pseudomonas aeruginosa</u> , Summary of the Results	73

LIST OF FIGURES

Figure	Page
1. Definition of processes during early colonization of a substratum	11
2. Experimental system	26
3. Results from a laser light scatter measurement on copper.	37
4. Cell accumulation of <u>Pseudomonas aeruginosa</u> on copper	38
5. Cell accumulation of <u>Pseudomonas aeruginosa</u> on silicon.	40
6. Results from a laser light scatter measurement on stainless	41
7. Cell accumulation of <u>Pseudomonas aeruginosa</u> on stainless.	42
8. Adsorption velocity of <u>Pseudomonas aeruginosa</u> versus surface roughness	44
9. Cell accumulation of <u>Pseudomonas fluorescens</u> (mot+) on stainless	45
10. Cell accumulation of <u>Pseudomonas fluorescens</u> (mot+) on polycarbonate	46
11. Cell accumulation of <u>Pseudomonas fluorescens</u> (mot+) on glass	46
12. Cell accumulation of <u>Pseudomonas fluorescens</u> (mot-) on stainless	49
13. Cell accumulation of <u>Pseudomonas fluorescens</u> (mot-) on polycarbonate	49
14. Cell accumulation of <u>Pseudomonas fluorescens</u> (mot-) on glass	50
15. Photograph, plate count on R2A agar	52
16. Cell Concentration Versus Duration of Starvation.	53
17. Cell Size Distribution Versus Duration of Starvation.	53
18. Adsorption Velocity Versus Duration of Starvation	55
19. Probability of Desorption versus Duration of Starvation	55
20. Simulation of cell accumulation of <u>Pseudomonas aeruginosa</u> on stainless at various bulk water cell concentrations.	59
21. Simulation of cell accumulation of <u>Pseudomonas aeruginosa</u> on stainless at various shear stress.	59
22. Simulation of cell accumulation of <u>Pseudomonas aeruginosa</u> on stainless, copper, and silicon at rich nutrient	60
23. Simulation of cell accumulation of <u>Pseudomonas aeruginosa</u> on stainless, copper, and silicon at low nutrient	60
24. Simulation of cell accumulation of a mixed population	61
25. Comparison of adsorption velocity of <u>Pseudomonas aeruginosa</u> on various substrata	63
26. Comparison of reversible and irreversible adsorption velocity	68
27. Cell surface hydrophobicity	68
28. Cell accumulation, chemostat effluent $D = 0.2 \text{ hr}^{-1}$	88
29. Cell Accumulation, 48 Hours of Starvation	88

LIST OF FIGURES (Continued)

Figure	Page
30. Cell Accumulation, 72 Hours of Starvation	89
31. Cell Accumulation, 120 Hours of Starvation	89
32. Cell Accumulation, 168 Hours of Starvation	90
33. Cell Accumulation, 216 Hours of Starvation	90
34. Cell Accumulation, 348 Hours of Starvation	91
35. Cell Accumulation, 504 Hours of Starvation	91
36. Cell Accumulation, 648 Hours of Starvation	92
37. Cell Accumulation, 816 Hours of Starvation	92
38. Cell Accumulation, 936 Hours of Starvation	93
39. Cell Accumulation, 1224 Hours of Starvation	93

ABSTRACT

The processes leading to bacterial accumulation on solid-water interfaces are adsorption, desorption, growth, and erosion. These processes have been measured individually in-situ in a flowing system and in real time using image analysis. The flow was laminar ($Re = 1.4$) and the shear stress was kept constant during all experiments at 0.75 Nm^{-2} . Five different substrata -- copper, silicon, 316 stainless steel, glass, and polycarbonate -- and three different bacterial strains -- Pseudomonas aeruginosa, Pseudomonas fluorescens (mot+) and Pseudomonas fluorescens (mot-) -- were used in the experiments. The surface roughness varied among the substrata from 25 Å for silicon as the smoothest substratum to 150 Å for copper as the roughest substratum. The effects of nutrient limitation and starvation of cells on sorption phenomena were also examined.

Sorption related processes were found to be influenced by the surface properties of the substrata and by the nature of the bacterial strain. Adsorption velocity was positively correlated with the surface roughness of the substratum and the surface hydrophobicity of the cells. While the sticking efficiency of a non-motile strain was found to be much higher than the corresponding motile strain, the motile cells adsorbed more rapidly due to superior transport properties arising from motility. Starvation of Pseudomonas aeruginosa cells was observed to result in a lower sticking efficiency, but increased motility resulting from dwarfing/fragmentation of the cells. Copper was found to inhibit cell growth on its surface, but the metal oxide layer on the surface as well as an already formed biofilm protected the cells and replication was observed after a longer exposure time to cell-containing bulk water. A mathematical model was developed to predict cell accumulation on a substratum, based on kinetic data for adsorption, desorption, growth, and erosion, for each of the tested substrata and organisms.

INTRODUCTION

The individual processes contributing to biofilm accumulation and activity must be understood and quantified in order to provide rational methodologies for their control or enhancement. A crucial initial event in biofilm accumulation is the adsorption of bacteria cells at a substratum. If these adsorbed cells find suitable environmental conditions, they will replicate, grow, and finally form a biofilm. The thickness of that film can vary from a single cell layer to several hundred millimeters as found in algae mats (Escher 1986). Biofilms not only cause biocorrosion but can also increase the resistance in heat exchangers, reduce flow rate in pipes, increase the drag of a ship, or cause pathogenic problems in municipal water supplies and food processing (Characklis and Marshall, 1990). In waste water treatment, biofilms are used as matrix for immobilizing microorganisms (Stevens and Crawford, 1990). Cell concentrations in biofilms are three to four orders of magnitude higher than those for planktonic cells. 10^{12} cells cm^{-3} is commonly found within biofilms, whereas 10^8 to 10^9 cells ml^{-1} are the maximum concentration for cells in suspension (Characklis and Marshall, 1990). Hence, biofilm systems allow not only higher dilution rates but also higher loading rates than conventional water or waste water treatment systems.

Bacterial growth in many natural habitats is limited by the availability of carbon or other substrates (Marshall 1985). In oligotrophic environments, the flux of substrates to the cells is of importance (Kjelleberg et al. 1983). An oligotrophic environment was

defined by Pointexter (1981) as a habitat with flux of $1 \text{ gC m}^{-3} \text{ day}^{-1}$ substrate or less. In these low nutrient environments, attachment of organisms to surfaces may be of particular advantage due to increased flux of nutrients to immobilized cells in comparison to planktonic organisms (Kjelleberg & Hermansson 1984). If nutrient concentrations are sufficiently low, starvation may occur (Morita 1982). Questions that may be asked are: Is adsorption to surfaces of any significance to starved bacteria? How is adsorption of a specific bacterium influenced by the duration of starvation? Is adsorption used as a strategic response to starvation for increasing the chances of survival by increasing nutrient flux?

Measuring only the accumulation of cells does not provide sufficient information to control, predict, or simulate a specific system. Therefore, bacterial colonization on a substratum has to be distinguished between the single contributing processes, such as adsorption, desorption, growth, and erosion. With a knowledge of the rate coefficient and reaction order for each of these processes, colonization at the solid-liquid interface can be characterized and simulated. Then, simulation models can be used to predict cell accumulation on different substrata under various environmental conditions. These models for initial colonization can be combined with existing models for mature biofilms, so that the complete development of a biofilm could be predicted and simulated.

This study continued the work of Escher (1986). Escher used image analysis to determine the influence of shear stress on early bacterial surface colonization in a laminar flow system at various bulk water cell concentrations. Pseudomonas aeruginosa was the test organism and a smooth

glass surface was the substratum.

Goal of Research

Characterize early bacterial colonization in a continuous flow system for various solid-water interfaces, environmental conditions, and microbial species.

Objectives of Research

1. Determine the rate of early bacterial colonization of Pseudomonas aeruginosa for various solid-water interfaces, such as copper, silicon, 316 stainless steel, glass, and polycarbonate.
2. Compare the rate of colonization of two different bacterial species (Pseudomonas aeruginosa and Pseudomonas fluorescens) as well as flagellated cells (mot+) and unflagellated cells (mot-) of Pseudomonas fluorescens.
3. Determine the relative effects of rich nutrient conditions with conditions of starvation on colonization rates.
4. Mathematically simulate early surface colonization at various solid interfaces, shear stress, and nutrient conditions for pure cultures and mixed populations.

BACKGROUND

Overview

The number of cells accumulating at the substratum will depend on many variables which can be categorized as surface properties at the solid-water interface, hydrodynamics, water chemistry, and microbiological. Temperature, pH, substrate concentration in the bulk liquid, the presence of trace elements and other nutrients such as phosphate and nitrogen and their ratio to carbon, the ionic strength of the bulk liquid, the coating of the surface, the substratum material, the substratum free surface energy (as reflected by hydrophobicity and surface roughness), as well as cellular properties might all influence the rates processes leading to bacterial accumulation on a solid-liquid interface (Abbott et al. (1983), Hermansson and Marshall (1985), Pedersen et al. (1986), Paul and Jeffrey (1985), Fletcher, (1980)).

Previous Research

The results reported by various researchers related to early events of bacterial surface colonization are not always consistent. Almost all research found in literature on early bacterial colonization on solid-liquid interfaces was done very carefully with respect to microbial, chemical, biochemical, and physico-chemical aspects. Unfortunately most of the reported research did not differentiate between adsorption, desorption, or growth on surfaces, but measured only cell accumulation.

Very little work can be found on hydrodynamic influences on bacterial colonization.

Bowen, Levine and Epstein (1976) proposed an analysis to describe the cellular transport rate to the substratum for a continuous flowing system and laminar flow conditions. Escher (1986), as well as Powell and Slater (1984), used image analysis to study the colonization behavior of bacteria cells on a smooth glass substratum under laminar flow. Powell and Slater used Bacillus cereus to study cellular adsorption in a glass capillary at laminar flow and compared their experimental results with theoretically calculated deposition rates for non motile cells when using Bowen's model. Escher used Pseudomonas aeruginosa as a test organism and varied bulk water cell concentration and fluid shear stress and determined the kinetic rates responsible for early cell colonization. By using Bowen's model, sticking efficiency and particle capture factor were calculated. Escher concluded that sorption related processes can be described as first order rates with respect to cell concentration in the bulk liquid and zero-order rates with respect to surface cell density. Growth related processes were found to be first order with respect to surface cell density.

Surface Free Energy

Inorganic solids with high melting points such as glass, metal, or silicon have high surface free energies ($500 - 5000 \text{ erg cm}^{-2}$). Soft organic solids with low melting points usually have surface energies less than 100 erg cm^{-2} (Zisman 1964). The main forces which contribute to the surface free energy are dispersion, dipole, electrostatic, and metallic

interactions.

Electrostatic charge may also be of importance for bacterial adsorption (Fletcher, 1980). The adsorption of organic substances may reduce the surface free energy. Adsorption of any organic material on surfaces will be determined by the free surface energy of the solid phase and the surface tension of the liquid phase (Fletcher, 1980). Similarly, adsorption and movement of bacteria at solid-liquid interfaces should be influenced by interfacial tension and bacterial surface properties. The free energy of solids can be determined by measuring the contact angle of water to the surface (θ), also called hydrophobicity of the wetted surface.

Surface Roughness

Surface roughness is mainly a function of the surface history (the way the surface was worked: machine worked, mechanically polished, electrochemically polished, etched etc). The cosine of the contact angle (θ) of the solid interface to water (surface hydrophobicity) is directly proportional to the surface roughness (Bikerman, 1970). Every groove, valley or scratch on a solid interface acts as a capillary tube in which the liquid rises as long as $\theta < 90^\circ$ or descends when $\theta > 90^\circ$. Thus a rough surface tends to exaggerate the wetting behavior of a solid (Adamson, 1960). When the contact angle of a smooth surface is small, it is even smaller on a rough solid of identical material.

Vanhaecke et al. (1990) tested six different Pseudomonas aeruginosa strains in a stagnant system and measured cellular accumulation on different polished stainless steel surfaces (electropolished and 120 grit

treated) after 30 minutes of exposure. The authors reported a drastic influence of surface roughness to the rate of cellular adsorption for Pseudomonas aeruginosa strains with a low cell surface hydrophobicity. For the strains with high hexadecane partitioning values the influence of surface roughness was reported to be minimal.

Hydrodynamic Factors

Escher (1986) was one of the few studies found which distinguished very carefully between adsorption, desorption, growth, and erosion to describe cell accumulation. He used Pseudomonas aeruginosa in a laminar flow system and varied fluid shear stress while keeping all the other parameters constant. Shear stress controlled the process of cellular colonization with a negative exponential influence on the rate of cell adsorption and cell separation. The rate of desorption was found to be independent of shear stress.

Chemical Factors

Calcium and magnesium ions positively influence bacterial adsorption (Turakhia 1986). Other complex organic compounds like EDTA or polymers have been shown to inhibit microbial adhesion (Marshall, 1972) simply by converting a favorable hydrophobic surface into an unfavorable hydrophilic surface. Stanley (1983) found an adsorption maximum at stainless steel for viable cells, both motile and non-motile at pH 7 to 8, whereas non viable cells adsorbed best at low pH values (pH 2 to pH 3). The same author found an increase in adsorption for Pseudomonas aeruginosa to stainless steel with increasing CaCl_2 or NaCl concentration in the bulk water. Vanhaecke

et. al. (1990) determined cell accumulation of Pseudomonas aeruginosa on stainless steel. They found cell surface hydrophobicity and surface roughness on the substratum were the major parameters influencing the rate of cellular adsorption but found no correlation between salt concentration and adsorption.

Microbiological Factors

Vanhaecke et al. (1990) reported a curvilinear positive correlation between cell surface hydrophobicity and cellular adsorption to 316-L and 304 stainless steel for 15 different Pseudomonas aeruginosa strains. Cell surface hydrophobicity was measured as bacterial adherence to hydrocarbons (BATH-test). Also, bacterial adsorption is affected by the nutrient available to the organisms. Kjelleberg, Marshall and Hermansson (1985) reported a relatively higher rate of adsorption to smooth glass substrata for marine bacteria grown in a low nutrient environment than for those grown in high nutrient environments. However, no significant differences were reported for the tendency of irreversible binding of the cells to surfaces. Bacterial adsorption may also depend on the type of limiting nutrient (e.g. carbon, oxygen, phosphate or nitrogen) (Brown et al. 1977).

Nutrient Availability - Starvation

In low nutrient environments bacteria on surfaces have selective advantages for growth and survival over planktonic cells. Cells need not be firmly attached to a substratum in order to benefit from the nutrient enriched state at the solid-liquid interface (Marshall 1978). In continuous flowing systems, an additional benefit is a higher nutrient

flux for adsorbed bacteria because there is no diffusion limitation of nutrient uptake. Marshall also reported regrowth to a normal size of small dwarf like bacteria within 12 to 20 hours after surface colonization.

Kjelleberg (1983) reported fragmentation and continuous size reduction (dwarfing) as a response to the initial phase of starvation. In Kjelleberg's experiment, the irreversible adsorption of Pseudomonas sp. strain S9 (hydrophobic) and Vibrio sp. strain DW1 (hydrophilic) increased during 4 hours of starvation. Kjelleberg (1984) did a similar experiment with seven marine isolates and found a small increase in irreversible adhesion after 5 hours followed by a small decrease after 22 hours of starvation for six strains. For one strain, the irreversible binding remained constant.

THEORY

Process Analysis at the Solid-Liquid Interface

Mathematical modeling attempts to describe real system behavior with a set of mathematical equations. Abiotic variables describe the physical and chemical environment in which the microbial process is occurring. Process Analysis combines these variables in mass, energy and momentum balance equations with stoichiometry, reaction rate, and transport coefficients to form predictive models. These coefficients vary with environmental parameters, such as temperature, pH, concentration of trace elements, the composition and balance of essential nutrients and its ratio to carbon, the ionic strength, the presence or absence of specific ions, such as calcium and magnesium.

There are several processes occurring during cellular colonization on a solid-liquid interface which must be distinguished. For mature biofilms, growth, erosion, detachment, and sloughing are the rate controlling processes. Initial events in biofilm accumulation are substratum conditioning by organic molecules and subsequent adsorption of cells (Characklis and Marshall, 1990). Some of these adsorbed cells will stay on the surface (irreversibly adsorbed cells) while others may desorb after some time (reversibly adsorbed cells). Kefford and Marshall (1984) suggested a model for the irreversible cell adsorption of Leptospira, where reversible adsorbed cells become irreversible adsorbed to a substratum after a certain time period. The cell surface binding mechanisms were found to be chemically different for reversibly and

irreversibly adsorbed cells. Escher (1986) reported a time interval between initial adsorption and desorption of *Pseudomonas aeruginosa* cells of 0.93 hr and a decreasing probability of desorption over the residence time of adsorbed cells with a high probability of desorption during the first 5 to 10 minutes. If a cell remained longer than 0.93 hours adsorbed on a substratum it was termed irreversibly adsorbed. Irreversibly adsorbed cells will replicate under suitable environmental conditions and the daughter cells may either desorb - erosion - or also become irreversibly adsorbed .

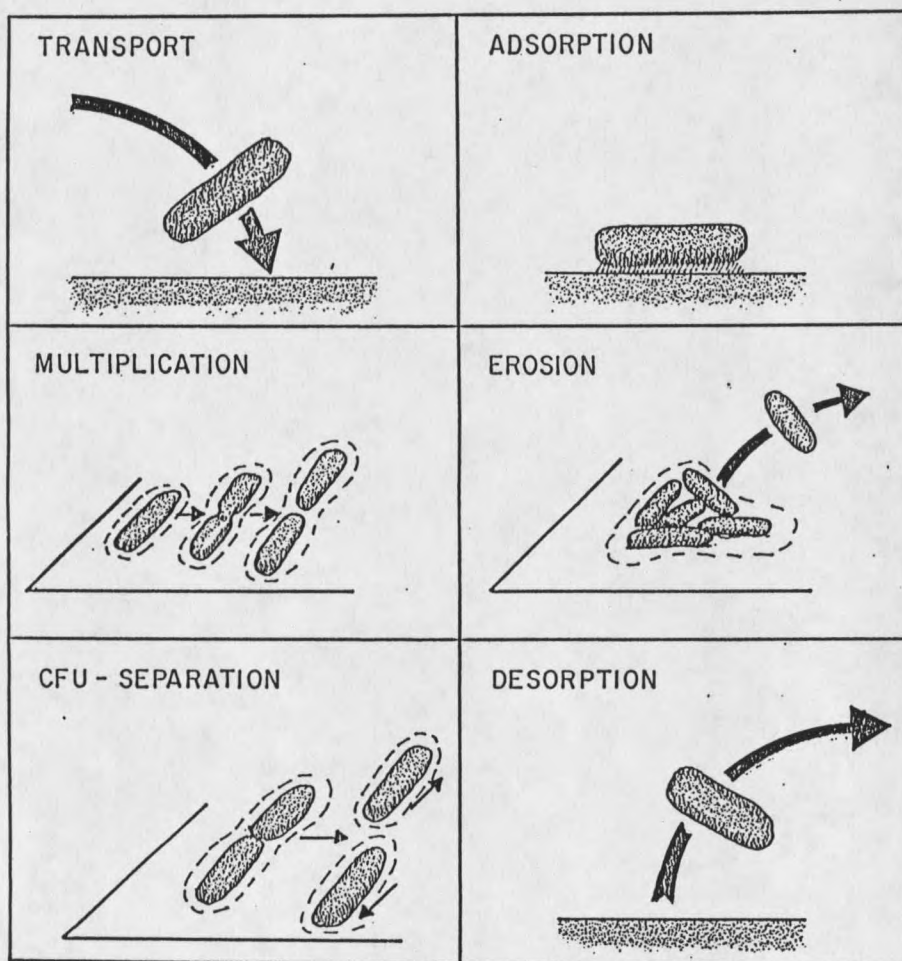


Figure 1. Definition of processes during early colonization of a substratum (Escher 1986)

The processes occurring at the solid-liquid interface could be distinguished between (Figure 1):

- Transport from the bulk water phase to the solid-liquid interface
- Adsorption on the substratum
- Desorption from the substratum to the bulk water phase
- Replication of irreversible adsorbed cells
- Erosion of cells from adsorbed colonies to the bulk water phase

Rate Coefficients of Early Surface Colonization

The rate coefficients were determined by using differential equations to express the quantitative, individual relationships of adsorption, desorption growth, and erosion at the interface:

$$r_a = K_a * X_b' \quad (1)$$

$$r_g = K_g * X'' \quad (2)$$

$$r_e = K_e * X'' \quad (3)$$

$$r_{airr} = f_{irr} * K_a * X_b' \quad (4)$$

$$f_{irr} = (1 - b) \quad (5)$$

$$f_{irr} = \frac{X_{irr}''}{X_{rev}''} \quad (6)$$

- X_b' : cell concentration in the bulk water [cell# L⁻³]
 X'' : cell surface density at time t [cell# L⁻²]
 X_{rev}'' : cell surface density of reversibly adsorbed cells at time t [cell# L⁻²]
 X_{irr}'' : cell surface density of irreversibly adsorbed cells at time t [cell# L⁻²]
 r : rate of adsorption, growth, or erosion, respectively [cell# L⁻² t⁻¹]
 K_a : adsorption velocity [L t⁻¹]
 K_g : coefficient of growth on the surface [t⁻¹]
 K_e : coefficient of erosion [t⁻¹]
 f_{irr} : fraction of irreversibly adsorbed cells [-]
 b : probability of desorption [-]

t: time [t]

Equations 1, 2, 3, and 4 assume first order rates (Escher 1986) for adsorption, desorption, growth, and erosion. For growth and erosion, the rates are dependent of cell surface density (X'') and are independent of bulk water cell concentration (X_b'). The rates of adsorption, and desorption are dependent of bulk water cell concentration (X_b') but independent of cell surface density (X'').

Growth on Surfaces

Most populations in uninhibited systems grow exponentially as described by Equation 2 (assuming no adsorption or desorption):

$$X'' = X_0'' * e^{\mu t} \quad (7)$$

X'' : cell surface density at time t [cell# L⁻²]
 X_0'' : initial cell surface density [cell# L⁻²]
 μ : specific growth rate [t⁻¹]

An important constant for an exponentially growing system is the generation time or doubling time g ($X'' = 2X_0''$).

$$g = \frac{\ln 2}{\mu} \quad (8)$$

g : time necessary to double the population [t]

From experimental results with Pseudomonas aeruginosa in biofilms, Bakke et al. (1984) suggested that the growth rates of organisms in the biofilm and in the planktonic state are the same as long as the microenvironment of the cells is the same. This should also be valid for adsorbed cells during early surface colonization. The specific growth rate

has a hyperbolic dependency on substrate concentration which is most commonly described by the Monod equation.

$$\mu = \frac{\mu_{\max} S}{K_s + S} \quad (9)$$

μ_{\max} : maximum growth rate [t^{-1}]
 K_s : cellular growth saturation constant [$M L^{-3}$]
 S : substrate concentration [$M L^{-3}$]

$K_s = 2.0 \text{ g m}^{-3}$ for *Pseudomonas aeruginosa* grown on glucose (Robinson 1984). When the maximum growth rate on a surface is known, Equation 9 could be used to calculate the specific growth rate for various nutrient conditions.

Cell Balance at the Substratum-Bulk Water Interface

The observed accumulation of cells on a substratum is dependent on adsorption rate, desorption rate, generation rate, and erosion rate:

$$\begin{array}{cccccc} \text{-----} & & & & & \\ \text{accumulation} & = & \text{adsorption} & - & \text{desorption} & + & \text{generation} & - & \text{erosion} & & (10) \\ \text{rate} & & \text{rate} & & \text{rate} & & \text{rate} & & \text{rate} & & \\ \text{-----} & & & & & & & & & & \end{array}$$

The rate of cell accumulation on a substratum can be expressed with the rate coefficients of sorption, growth and erosion:

$$\frac{dX''}{dt} = f_{irr} * K_a * X_b' + K_g * X'' - K_e * X'' \quad (11)$$

Equation 11 does not have individual terms for death and decay of the adsorbed cells. These rates are included in growth and erosion. The rates describing bacterial colonization are measured at constant

environmental conditions as rate of growth, rate of erosion, rate of adsorption, and desorption. The kinetic coefficients were determined by regression analysis. The rate coefficients determined are not maximum rates but dependent on temperature, substratum, nutrient concentration, hydrodynamics in a system, etc.. Equation 11 was used as basic equation for all the surface colonization simulations presented in this study.

Process Analysis for Chemostat Operation

In a chemostat, mixing is assumed to be ideal and biofilm growth on the walls is neglected. When operating a chemostat under steady state condition, the number of cells in the effluent is constant. Thus, a chemostat was chosen to control cell concentration for all experiments in this study. With dilution rate smaller than the maximum growth rate, an ideal chemostat can be described by the following equations, assuming a sterile influent ($X_i = 0$) and steady state conditions:

$$\mu = Q/V \quad (12)$$

$$X = Y*(S_i - S) \quad (13)$$

- Y : yield [$M M^{-1}$]
 X : biomass concentration in chemostat [$M L^{-3}$]
 S : substrate concentration in chemostat [$M L^{-3}$]
 S_i : influent substrate concentration [$M L^{-3}$]
 V : volume of chemostat [L^3]
 Q : influent/effluent flowrate [$L^3 t^{-1}$]

To convert biomass into cell numbers a conversion, including cell size and cell density has to be used:

$$X = X_c' \rho_{cell} V_{ac} \quad (14)$$

X_c' : chemostat effluent cell concentration [cell# L⁻³]
 ρ_{cell} : average cellular density [M L⁻³]
 V_{ac} : average cell volume [L³]

The cellular density is fairly constant for most of the pseudomonads with a wet cell density of $\rho_{cell} = 1.004 \cdot 10^{-3}$ g mm⁻³ (Characklis and Marshall, 1990). The average cell volume was determined by image analysis for Pseudomonas aeruginosa and Pseudomonas fluorescens ($\mu = 0.2$ hr⁻¹):

$$V_c(av) = 0.675 \pm 0.105 \mu\text{m}^3$$

For starved cells of Pseudomonas aeruginosa, and starved cells of Pseudomonas fluorescens:

$$v_c(av) = 0.355 \pm 0.095 \mu\text{m}^3$$

Modified Chemostat Operation for Starvation

To study starvation of microbial cells, the chemostat influent flow was terminated. Therefore, the chemostat was changed into a batch reactor. Inactive microbial mass was generated because some cells died and lysed as a result of endogenous metabolism and did not contribute to substrate removal. Death and lyse rate are generally treated as first order with respect to viable and dead cell biomass, respectively. Processes occurring in a batch reactor with only one bacteria species can be described by the following equations, assuming substrate removal is attributed only to the active, viable cells and also assuming that only dead cells will lyse:

$$\text{Substrate balance: } \frac{dS}{dt} = - \frac{\mu X_v}{Y} \quad (15)$$

$$\text{Biomass balance: } \frac{dX_t}{dt} = \mu X_v - k_l (X_t - X_v) \quad (16)$$

(total cells)

$$\text{Biomass balance: } \frac{dX_v}{dt} = (\mu - k_d) X_v \quad (17)$$

(viable cells)

$$\text{Biomass balance: } \frac{d(X_t - X_v)}{dt} = k_d X_v - k_l (X_t - X_v) \quad (18)$$

(non-viable cells)

- X_t : total biomass concentration [M L⁻³]
 X_v : viable biomass concentration [M L⁻³]
 k_d : death rate with respect to viable cell concentration [t⁻¹]
 k_l : lyse rate with respect to non-viable cell concentration [t⁻¹]

The specific growth rate (μ) in biochemical systems is best described by the empirical Monod equation (Equation 9). At low substrate concentrations, the specific growth rate is directly proportional to the substrate concentration but independent of it at high concentrations. In the case of starvation ($S \ll K_s$), a first order expression results:

$$\mu = \frac{\mu_{\max} S}{K_s} \quad (19)$$

After an even a short starvation period, lysed cells would be the only available carbon source, other additional carbon sources having been depleted in the system. With the assumption that all the carbon from lysed cells is available as nutrient for the remaining viable cells the substrate balance (Equation 15) can be modified as follows:

$$\frac{dS}{dt} = - \frac{\mu X_v}{Y} + F k_l (X_t - X_v) \quad (20)$$

F : gravimetric cell factor, carbon content per biomass [M M⁻¹]

Assuming that the change in substrate concentration will approach zero after a long duration of starvation, Equation 20 can be solved for lyse rate (k_l) by substituting Equation 19 for μ . Simultaneously, Equation 16 can be solved for death rate (k_d):

$$k_d = \frac{\mu_{\max}}{K_s Y F} \frac{S}{(X_t - X_v)} \quad (21)$$

$$k_d = \frac{\mu_{\max} S}{K_s} + \frac{1}{X_v} \frac{dX_v}{dt} \quad (22)$$

With Equation 21 and 22, lyse rate and death rate can be determined by following only three parameters versus duration of starvation: viable and total cell concentration and the substrate concentration (dissolved organic carbon) in the water phase. With Equation 14, biomass concentration can be converted into cell concentration.

Transport

Diffusivity for Motile Cells

Diffusion is the main transport process perpendicular to the direction of flow for small particles such as bacteria cells under laminar flow conditions. Jang and Yen (1985) used the following equation to calculate diffusivity for various organisms:

$$D_c = \frac{v_r * d_r}{3 * (1 - \cos\alpha)} \quad (23)$$

- D_c : diffusivity [$L^2 t^{-1}$]
 v_r : velocity of motility [$L t^{-1}$]
 d_r : free length of random run [L]
 α : main angle of turn; assuming no chemotaxis $\cos\alpha = 0$

Equation 23 enables the calculation of non-Brownian diffusivity from cellular motility data for a specific species. Escher (1986) pointed out that diffusion by Brownian motion can be neglected relative to motility.

He calculated non Brownian diffusivity of Pseudomonas aeruginosa from data obtained by Vaituzi and Doetsch (1969) ($v_r = 55.8 \mu\text{m s}^{-1}$; $d_r = 50-85 \mu\text{m}$) as $10^{-3} \text{ mm}^2 \text{ s}^{-1}$.

Kim (1990) determined diffusivity of Pseudomonas aeruginosa experimentally, by using a capillary tube method. He used an equation which was derived by Segel et al. (1977) assuming that for a long enough capillary tube with a small cross-sectional area, diffusion can be described by a material balance in one dimension:

$$D_c = \frac{\pi N^2}{4 X_0'^2 A^2 t} \quad (24)$$

- N : total number of cells in the tube [cell#]
 X_0' : suspended cell concentration [cell# L⁻³]
 A : cross-sectional area of the tube [L²]

Kim reported a value of $2.1 \cdot 10^{-3} \text{ mm}^2 \text{ s}^{-1}$ and a standard deviation of $1.3 \cdot 10^{-3} \text{ mm}^2 \text{ s}^{-1}$ for non Brownian diffusion of Pseudomonas aeruginosa.

Therefore, the values obtained from the calculation using Jang and Yen's equation match well with the experimental results from Kim using Segel's equation for a capillary tube.

Diffusivity of Non-Motile Cells

The Stokes-Einstein equation yields good estimates for diffusion coefficient of small particles or non motile bacteria cells but cannot be used for motile cells:

$$D_c = \frac{k_b T}{f} = \frac{k_b T}{6 \pi \mu_b R_A} \quad (25)$$

- k_b : Boltzman constant, $1.38062 \cdot 10^{-23} \text{ J K}^{-1}$.
 T : Temperature [T]
 μ_b : Viscosity of suspended medium [N t L^{-2}]
 R_A : Cell radius [L]
 f : cell factor [N t L^{-2}]

For rod shaped non motile cells with an average volume of $0.675 \mu\text{m}^3$ and a diameter to length ratio of 0.45 (for Pseudomonas species), the diffusivity calculated by the Stokes-Einstein Equation at 22°C is $3.9 \cdot 10^{-7} \text{ mm}^2\text{s}^{-1}$. Thus, calculated diffusivity for motile cells is almost 4 orders of magnitude higher than the calculated diffusivity for non-motile cells of the same size and shape.

Transport to the Solid-Liquid Interface

Bowen et al. (1976) proposed an analysis to describe particle deposition from a suspension at fully developed laminar flow in a parallel plate channel. They assumed a first order reaction rate at the wall and calculated the transport of small particles to a solid-liquid interface. The particle deposition rate is expressed by the following equation which converges well for large Peclet numbers:

$$K_a'' = \frac{X_b' D_c}{h} \frac{(2/9K_i)^{1/3}}{[\Gamma(4/3) + (1/\epsilon) \cdot (2/9K_i)^{1/3}]} \quad (28)$$

- K_a'' : flux of particles adsorbing to the substratum [$\# \text{ L}^{-2} \text{ t}$]
 X_b' : particle concentration in the bulk water [$\# \text{ L}^{-3}$]
 D_c : diffusivity [$\text{L}^2 \text{ t}^{-1}$]
 h : half-thickness of channel [L]
 K_i : dimensionless distance [-]
 ϵ : surface particle capture factor [-]
 Γ : gamma function [$\Gamma(4/3) = 0.89338$]

The authors limited their analytical solution to particles which are characterized by small Brownian diffusivities and large Peclet numbers. However, Equation 28 was used (Escher 1986) to describe cell transport from the bulk water to the solid interface for motile cells with high diffusivity values. Bowen's proposed analysis will, therefore, be used in this study to calculate sticking efficiency and particle capture factor, and tested by a comparison of motile and non motile cells of the same *Pseudomonas* strain.

The surface particle capture factor (ϵ) in Equation 27 can be described as a first order rate coefficient with respect to the bulk water cell concentration. Low values of ϵ indicate a low probability of adsorption, when the value of ϵ approaches infinity [$(1/\epsilon) = 0$] the surface acts like a perfect sink and Equation 27 becomes:

$$N_t'' = \frac{X_b' D_c}{h} \frac{(2/9K_i)^{1/3}}{\Gamma(4/3)} \quad (27)$$

N_t'' : total flux of particles to the substratum [# L⁻² t⁻¹]

Equation 27 describes the total flux of particles to the substratum. When measuring the rate of adsorption, the surface particle capture factor (ϵ) can be calculated from Equation 26 knowing the dimensionless distance K_i as:

$$K_i = Pe^{-1} \frac{8 x}{3 h} \quad (28)$$

Pe : Peclet number [-]
 x : Length from channel inlet [L]
 h : half thickness of channel [L]

The Peclet number is defined as follows:

$$Pe = \frac{4 v_m h}{D_c} \quad (29)$$

v_m : mean bulk velocity [$L t^{-1}$]

Adsorption Velocity

The adsorption velocity can be calculated by normalizing the flux of particles/cells to the substratum to the particle/cell concentration in the bulk water.

$$Ka = \frac{K_a''}{X_b'} \quad (30)$$

Ka : adsorption velocity [Lt^{-1}]

Adsorption velocity is independent of bulk water particle/cell concentration but dependent on geometry and hydrodynamics of the flow system and diffusivity and adsorption ability of the particles/cells. Ka can be calculated using the viable cell counts (Ka_v) as well as using the total cell counts (Ka_t). The adsorption velocity of irreversibly adsorbed cells can be expressed by:

$$Ka_{irr} = f_{irr} Ka \quad (31)$$

Ka_{irr} : adsorption velocity of irreversibly adsorbed cells [$L t^{-1}$]

Adsorption velocity could be used to compare bacterial adsorption for various substrata or organisms for constant flow conditions and geometry in the flow system.

Sticking Efficiency

Sticking efficiency is defined (Characklis and Marshal, 1990) by the ratio of cells adsorbing to the substratum to the number of cells colliding with the substratum. Sticking efficiency can be used as a system independent parameter to compare bacterial adsorption at various interfaces or environments. The sticking efficiency can be expressed as follows:

$$\text{Sticking efficiency} = \frac{K_a''}{N_t''} \quad (32)$$

K_a'' and N_t'' are described in Equation 26 and 27, respectively. Sticking efficiency could be expressed in the ratio of these two Equations:

$$\Phi = \frac{\Gamma(3/4)}{\Gamma(3/4) + (1/\epsilon)(2/9K_i)^{1/3}} \quad (33)$$

Φ : sticking efficiency [-]

Sticking efficiency is a function of the particle capture factor and the Peclet number but independent of cell concentration. The values for Φ will vary between 0 and 1. High values for Φ indicate a high tendency for the cells to adsorb to a substratum, while low values of Φ indicate a low tendency of cells to adsorb to a substratum. It should be emphasized that a high value for sticking efficiency does not necessarily correspond to a high adsorption velocity, because sticking efficiency is independent of the transport properties of the cells.

Fluid Dynamics

For fully developed laminar flow in a Newtonian fluid, shear stress can be calculated by Newton's law of viscosity. With a direction of flow in y-direction and an even flow distribution in x-direction, the shear stress is given by:

$$\tau_{zy} = - \mu_w \frac{dv_y}{dz} \quad (34)$$

- τ_{zy} : shear stress [N L⁻²]
 μ_w : fluid viscosity [N t L⁻²]
 v_y : bulk liquid velocity [L t⁻¹]
 y : length coordinate in axial direction [L]
 z : height coordinate normal to the flow [L]

At the center of the flow channel $z = 0$; $v_y = v_{\max} = 3/2 v_m$ and $dv_y/dz = 0$; at the walls $z = \pm h$ and $v_y = 0$. In a fully developed laminar flow between two parallel plates the velocity profile has a parabolic shape (Bowen et al. 1976):

$$v_y(z) = 3/2 v_m (1 - z^2/h^2) \quad (35)$$

shear stress at the wall:

$$\tau_{\text{wall}} = - 3/2 \mu_w v_m h^{-1} \quad (36)$$

- τ_{wall} : shear stress at the wall [N L⁻²]
 h : half-thickness of Channel [L]
 v_m : mean bulk velocity [L t⁻¹]

When the mean bulk water velocity is much larger than cellular motility, the hydraulic detention time of cells above the substratum can

be determined as a function of their location:

$$\text{HRT}(z) = \frac{2l_s}{3v_m [1 - (z^2/h^2)]} \quad (37)$$

- l_s : length of substratum [L]
 HRT : hydraulic detention time of cells above the substratum [t]

The cellular detention time is a function of bulk water velocity and the cell location at the entrance perpendicular to the substratum.

Reynolds Number

The Reynolds number is commonly used to categorize flow conditions in closed conduits as laminar or turbulent. If the Reynolds number is smaller than 2100 the flow is called laminar. For values greater than 2100 the flow is said to be turbulent. Reynolds number depends mainly on the mean bulk water velocity and the geometry of the flow system and is defined as follows:

$$\text{Re} = \frac{2 R_h v_m \rho_w}{\mu_w} \quad (38)$$

$$R_h = \frac{A}{Z} \quad (39)$$

- Re : Reynolds number [-]
 v_m : mean bulk water velocity [L t⁻¹]
 ρ_w : density of water [M L⁻³]
 μ_w : fluid viscosity [N t L⁻²]
 R_h : hydraulic radius [L]
 A : cross sectional area [L²]
 Z : wetted perimeter [L]

METHODS

Experimental System

The experimental system was used as described by Escher (1986) (Figure 2). Bacterial cells were grown in a chemostat (330 ml volume) until steady state conditions were reached. A phosphate buffered glucose solution was used as nutrient (Table 1). Growth in all experiments was carbon limited (40 g m^{-3} as TOC) and buffered at pH 6.8. Because of a relatively high cell concentration in the chemostat, the effluent was diluted with dilution water before entering the flow cell. The dilution water had the same chemical composition as the nutrient except that no organic carbon was present.

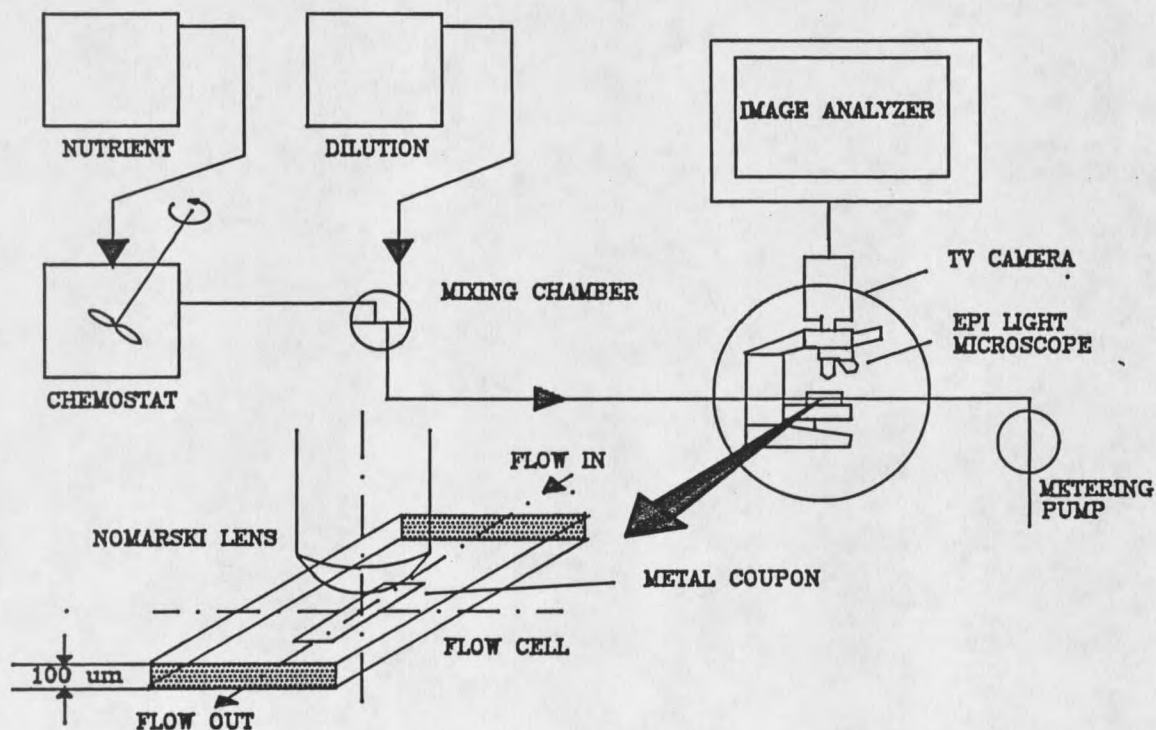


Figure 2. Experimental system

Table 1. Chemical composition of nutrient.

Chemical	Concentration in g m^{-3}
Glucose	100
NH_4Cl	36
Na_2HPO_4	568
KH_2PO_4	544
CaCO_3	90

Micronutrients were added according to Trulear (1983).

The diluted chemostat effluent was pumped by a non-pulsing gear pump at a constant flow rate through a flow cell (Table 2). All experiments were conducted in laminar flow at a shear stress of 0.75 N m^{-2} which corresponds to a flow rate of $1.2 \times 10^{-4} \text{ m}^3 \text{ hr}^{-1}$ and a mean bulk water velocity of $2.75 \times 10^{-2} \text{ m s}^{-1}$. For a shear stress of 0.75 N m^{-2} at the solid-water interface, the Reynolds number in the flow chamber was 1.4.

Table 2. System specific parameters for the flow cell used in the experiments.

length of flow cell	:	40.00	mm
length of metal coupon	:	26.50	mm
width of flow cell	:	12.10	mm
width of metal coupon	:	6.70	mm
height of flow channel	:	0.10	mm
cross sectional area	:	1.21	mm^2
bulk liquid flow rate	:	0.12	l hr^{-1}
bulk liquid mean velocity	:	0.0275	m s^{-1}
corresponding shear stress	:	0.75	N m^{-2}
mean cellular detention time	:	0.96	s

Coupons inserted at the bottom of the flow cell were used as substrata. The reflective coupon surfaces (copper, silicon, 316 stainless steel) were monitored continuously using reflective light from an EPI light microscope equipped with a Nomarski lens. Magnification was between

1000 and 1500. For lower magnifications, the light reflection from the surface was too disperse to obtain quantitative information of cell colonization. Transmitted light was used for monitoring transparent surfaces, such as glass or polycarbonate. The microscope output was linked to a video camera. The video signal was transferred to an image analysis system (IAS) which converted the grey image from the video camera into a binary image. The IAS counted the actual number of cells on the surface with respect to size and location. The cell measurement data could be stored to disk during experiments and retrieved for analysis at a later time. The use of the IAS to measure bacterial surface colonization is described in more detail by Escher (1986).

The metal coupons were mechanically polished so that light reflection enabled the observation of individual bacteria cells. "Buehler Alpha Micropolish II deagglomerated Alumina 1.0 and 0.3" were used in distilled water for polishing. This polisher has a hexagonal crystal structure and a particle size of 1.0 or 0.3 μm , respectively.

Pseudomonas aeruginosa and Pseudomonas fluorescence were the test organisms. Both Pseudomonas strains are strict aerobic, rod-shaped, polar flagellated, gram-negative cells, 1.0 to 2.5 μm long and 0.4 to 0.6 μm in diameter. The same Pseudomonas fluorescence strain was used in a modified mot- version (provided from D. E. Caldwell, Vancouver, British Columbia). The mot- mutant were found to lack a flagellum by transmission electron microscopy analysis (Korber et.al. 1989). There was no significant difference between the growth rate of Pseudomonas aeruginosa and Pseudomonas fluorescens of the mot+ parent and the mot- mutant in batch cultures ($\mu = 0.45 \text{ hr}^{-1}$), (Korber et. al. 1989).

Method of Analysis

Total Cell Count

The water samples (bulk water or chemostat effluent) were fixed in 2 % Formalin solution and stored at 4°C. All containers were autoclaved before use for sampling. For staining, the prepared sample was homogenized and suspended in 2 ml 0.01% acridine orange for 30 min. The stained sample was filtered through a 0.2 μm black filter and the cells were counted by image analysis using fluorescence light at 1000 x magnification. 10 fields on each filter were averaged to determine the cell concentration in the sample. Replicates of several filters with the same sample yielded a standard deviation of less than 10%.

Viable Cell Counts

A dilution series was made from the water sample. 0.1 ml from the dilutions was equally distributed on three replicate plates with R2A-agar as growth media. Replicates of several plates of the same sample showed a standard deviation between 7 and 15 %.

Cell Surface Hydrophobicity

This method is based on the degree of "bacterial adherence to hydrocarbons" (BATH) and has found application in the study of a wide variety of bacteria and bacterial mixtures (Rosenberg 1984). The method used (BATH-test) was developed by Rosenberg and co-workers (Rosenberg et. al. 1980) and was adapted for use with image analysis. Two ml of hydrocarbon (n-octane or n-hexadecane) were added to round bottom test

tubes containing 5 ml phosphate-buffered sample. P-xylene was originally suggested for use in the test, but was abandoned because it produced unreliable results. Others also reported problems with the use of p-xylene for measuring cell surface hydrophobicity (Vanhaecke, Pijck, 1988). Following 10 minutes of preincubation at 30 °C, the mixtures were homogenized for 2 minutes. The hydrocarbon phase was allowed to separate for 15 minutes, and the aqueous phase was removed with a pasteur pipette. Total cell concentration was performed for the initial bacteria mixture and the aqueous phase after hydrocarbon extraction. The decrease in cell concentration of the aqueous phase was used as a measure of cell surface hydrophobicity. Cell surface hydrophobicity is reported as the fraction of cells removed by hexadecane or octane, respectively, and is called hexadecane or octane partitioning value, respectively.

Total Organic Carbon (TOC)

TOC was measured using a Dohrman model DC 80 total organic carbon analyzer. The pH of the water sample was lowered to ph 2 with phosphoric acid, and aerated to strip all carbon dioxide from the sample. All samples were homogenized and analyzed by direct injection.

Dissolved Organic Carbon (DOC)

The measurements for filtered water samples were very inconsistent. Up to 10 ppm carbon was leached from the filter. The carbon contamination also varied considerably between filters. Especially for low carbon concentrations, it was difficult to obtain consistent results. The use of PTFE membranes with a pore size of 0.2 μm finally gave satisfying results

after rinsing for several (about 8 to 10) times with diluted phosphoric acid.

Surface Roughness

Surface roughness was obtained from reflected light scatter distribution by using a Raleigh perturbation relationship. A reflector power spectral density function (PSD) can be calculated from the light scatter at various reflection angles. In general, the calculated PSD behaves as a function of the surface topology. Integrating the PSD function gives the root mean square (RMS) surface roughness value (Stover, Serati, Gillespie 1984).

Estimation of Cell Motility

To estimate cellular motility, the substratum was exposed to the cell containing bulk water at a shear stress of 0.75 N m^{-2} until a cell surface density of approximately 4000 CFU mm^{-2} was reached. After initial adsorption occurred, the flow over the substratum was terminated. Within 5 to 10 minutes, most of the initially adsorbed cells became motile on the surface. The surface was monitored continuously at a magnification of 1500x and recorded by a high resolution VCR on video tape. The TV screen was calibrated by recording a calibration slide at the same magnification in horizontal and vertical direction. After replaying the tape several times, the random free runs could be measured by marking traveling phase (free run) and twiddling phase (change in traveling direction). When replaying the tape in slow motion with time control, the cellular swimming speed for a free run could be estimated (Korber et al., 1989).

The same procedure was used to test mot- cells for motility after cellular colonization.

Determination of Rate of Adsorption and Desorption on the Substratum

The rate of adsorption and desorption was measured by exposing the solid interface to a bulk water flow of constant cell concentration and shear stress (0.75 N m^{-2}). Individual cells were, counted and memorized with respect to their location and size on the substratum over time. When plotting the number of cells adsorbing or desorbing versus time linear regression analysis could give the values for adsorption velocity and the probability of desorption (Escher, 1986).

Determination of Rate of Growth and Erosion on the Substratum

The substrata were exposed to a bulk water flow (shear stress 0.75 N m^{-2}) of approximately $3 \cdot 10^6 \text{ cells ml}^{-1}$ until the cell surface density reached a value between 2000 and 3000 CFU mm^{-2} . These cells were adsorbed at an irreversible state. After this initial colonization period, approximately 30 minutes for copper to 2 hours for silicon, the bulk water flow was switched from the diluted chemostat effluent to a sterile nutrient solution of identical chemical composition as fed to the chemostat. The rate of growth on surfaces was determined by following individual cells replicating over time. Simultaneously, the rate of erosion could be determined by following individual cells desorbing from the surface. After plotting the number of cells replicated versus time, the growth rate and doubling time could be determined by regression

analysis.

Image Analysis

The Cambridge Q10, equipped with an image analyzer unit (68000 processor) was used in the experimental system. In addition to the display and output of the measurements, the image analyzer can perform limited statistical analysis. Up to eight different distribution histograms can be calculated at the same time. The instrument has two different routines, one in compiled C and one in M-Basic. Images were manipulated by a digipad connected to the image analyzer.

RESULTS

Results were obtained for five different materials and two different bacteria species - Pseudomonas aeruginosa and Pseudomonas fluorescens. Pseudomonas fluorescens was used as a mot+ strain as well as a mot- mutant. Substrata included copper, 316 stainless steel, silicon, glass and polycarbonate. The surface roughness varied with various material from 25 Å (2.7×10^{-3} μm) for silicon to 150 Å (15.6×10^{-3} μm) for Copper as the roughest surface used in the experiments. 316 stainless steel was used to perform a long duration starvation study (as long as 1224 hours).

Chemostat Operation

The chemostat was operated at a dilution rate of 0.2 hr^{-1} , and the chemostat effluent concentration varied between 3.8 to 4.5×10^7 cells ml^{-1} (measured as total count). The effluent dissolved organic carbon varied between 3.2 and 5.0 g m^{-3} . Before entering the flow chamber, the chemostat effluent was diluted to a factor of approximately 10 with carbon free and cell free dilution water. Hence, the dissolved organic carbon in the bulk water varied between 0.1 and 0.6 g m^{-3} and cell concentration in the bulk water was kept between 10^6 and 10^7 cells ml^{-1} . Temperature was controlled in the chemostat at $30 \text{ }^\circ\text{C}$ and the temperature at the solid-water interface was estimated to be constant at $22 \pm 2^\circ\text{C}$. Shear stress was kept constant during all experiments at 0.75 N m^{-2} in the flow chamber.

Image Processing

Images were taken at 10 minute intervals and manipulated by using the digipad drawing device. Regression analysis was applied to determine the rate coefficients for adsorption, desorption, growth and erosion.

Cell Surface Hydrophobicity

Cell surface hydrophobicity was measured as "bacterial adherence to hydrocarbons" (BATH-test, Rosenberg, et al, 1980). For all the tested cells, the hexadecane partitioning values were higher than the partitioning values for octane (Table 3). Mean hydrocarbon partitioning (cell surface hydrophobicity) values were calculated by averaging the hexadecane and octane partitioning values for each species and strain. The lowest carbonhydrate partitioning values were found for Pseudomonas fluorescens (mot+). The Pseudomonas fluorescens (mot-) strain had a significantly higher value for cell surface hydrophobicity than the motile strain. Pseudomonas aeruginosa was found to be highly hydrophobic.

Table 3. Cell surface hydrophobicity.

Strain	octane part. value (-)	hexadecane part. value (-)	mean HC part. value (-)
<u>Ps aeruginosa</u>	0.95±0.01	0.99±0.01	0.97±0.02
<u>Ps fluorescens</u> (mot+)	0.54±0.11	0.80±0.04	0.67±0.13
<u>Ps fluorescens</u> (mot-)	0.91±0.04	0.93±0.03	0.92±0.04

Pseudomonas aeruginosa, Kinetic Results

Surface Colonization of Pseudomonas aeruginosa

Pseudomonas aeruginosa cells were transported to the interface either as single cells or in a divided cell state (divided cells but not separated). Colonization occurred in the same manner. Clustering was not observed on the substratum and desorption occurred as single or divided cells from the substratum to the bulk water.

Copper

Copper corrosion results in a copper oxide layer within hours of exposure to air. The copper oxide layer has a protective function for the metal underneath. The presence of an oxide layer can be easily detected by visual observation. A freshly polished copper surface is shiny and reflective, whereas an oxidized copper surface looks dull and absorbs light. A fresh polished surface was important for reflective light measurements. Copper is a soft metal and polished very fast but was difficult to keep clean. The orientation of polishing was determined from a light scatter surface roughness measurement (Figure 3). The RMS surface roughness of a freshly polished copper coupon, when measured in vertical direction (direction of flow), was 220 Å, whereas the RMS surface roughness in horizontal direction (direction perpendicular to the flow) was 82 Å. Therefore, the orientation of dislocations (polishing tracks) were mainly in the vertical direction. For comparison with other reflective surfaces an average value was calculated (150 Å). After the

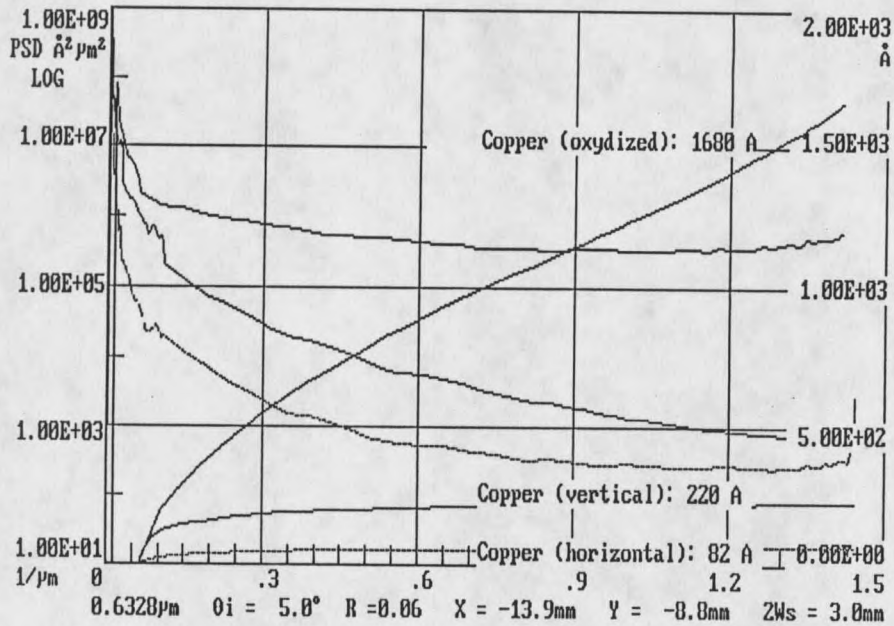


Figure 3. Results from a laser light scatter measurement on the copper surface. Power spectral density (PSD) is plotted versus frequency. The integration of this curves provide values for RMS surface roughness. A fresh polished copper surface, measured in vertical and horizontal direction is compared with a highly oxidized surface.

polished copper coupon was exposed to air for several weeks the RMS surface roughness increased to 1680 \AA .

Cell accumulation on the copper substratum was expressed as cell surface density (X'') and observed for a bulk water cell concentration of $1.50 \times 10^6 \text{ cells ml}^{-1}$ (Figure 4 a). The steep slope indicates a high rate of adsorption ($K_a = 2.23 \text{ mm hr}^{-1}$). The rate of desorption was rather low (probability of desorption $b = 0.10$). There was no replication of cells observed when using copper as substratum (Figure 4). Even for an extended period of time (24 hours) no replication was seen. However, if the exposure time to a cell suspension was long enough for a monolayer of cells to accumulate, replication of cells in the second and higher cell layers was observed. Unfortunately, an accurate measurement of growth rate

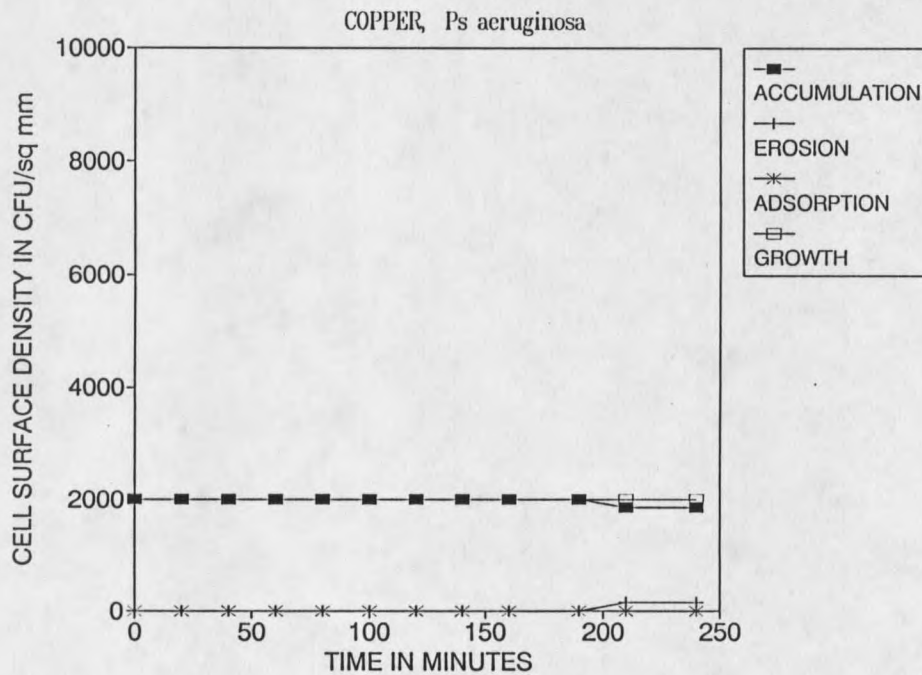
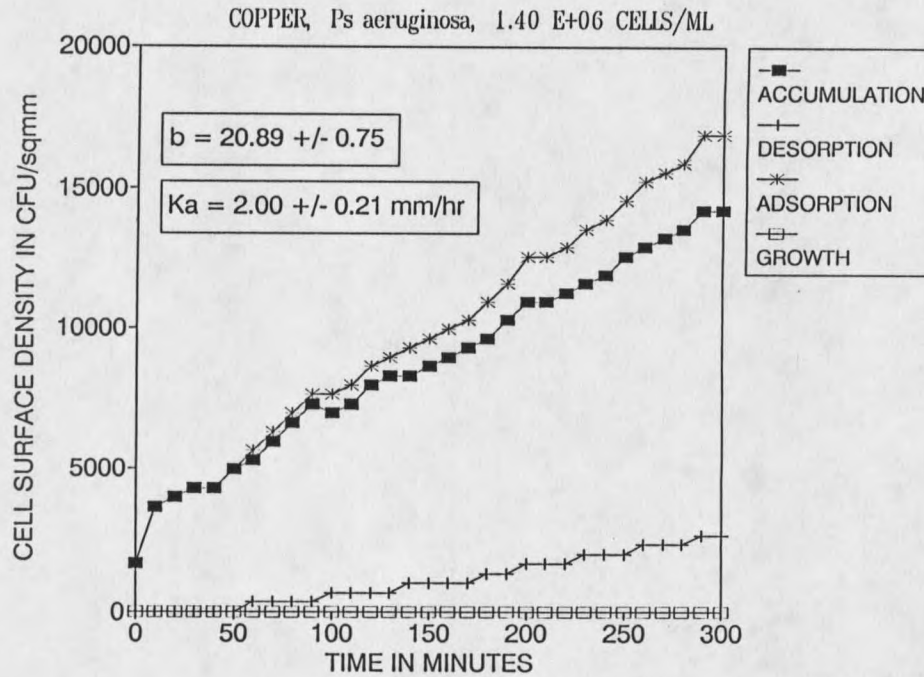


Figure 4. Cell accumulation of *Pseudomonas aeruginosa* on copper using a bulk water concentration of 1.4×10^6 cells ml^{-1} (Figure 4 a) and a sterile nutrient (40 ppm C) after initial cell colonization of 2000 CFU mm^{-2} (Figure 4 b). Shear stress 0.75 N m^{-2} .

in upper cell layers was technically not possible with the image analysis system. The kinetic results for Pseudomonas aeruginosa are summarized in Table 4.

Silicon

Silicon is used in industry as a semiconductor material mostly in its monocrystalline form. To allow very accurate photographic etching procedures, the silicon chips are thinly sliced and polished with high precision to very low surface roughness values and a high degree of flatness.

The monocrystalline silicon substratum had a RMS surface roughness of 25 Å without regard to its orientation. The bulk water concentration was constant during the accumulation experiment at 3.5×10^6 cells ml⁻¹ (Figure 5 a). The adsorption velocity was low ($K_a = 0.47$ mm hr⁻¹) and the probability of desorption was high ($b = 0.86$). Most cells did not remain at their location for an extended period of time after initial adsorption. The rate of erosion ($K_e = 0.32$ hr⁻¹) was slightly higher than the growth rate ($K_g = 0.28$ hr⁻¹) (Figure 5 and Table 4), hence the accumulation of cells on the silicon surface was slow. Even cells that were adsorbed for a long period of time (over 200 minutes) desorbed when additional shear was applied. Replication of adsorbed cells often resulted in desorption of both, mother and daughter cells .

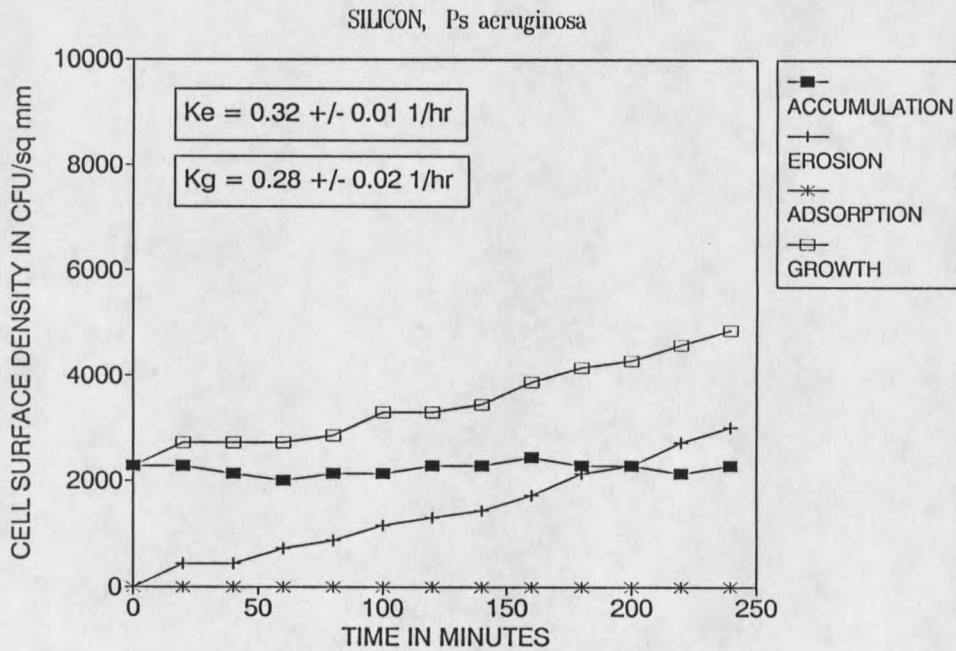
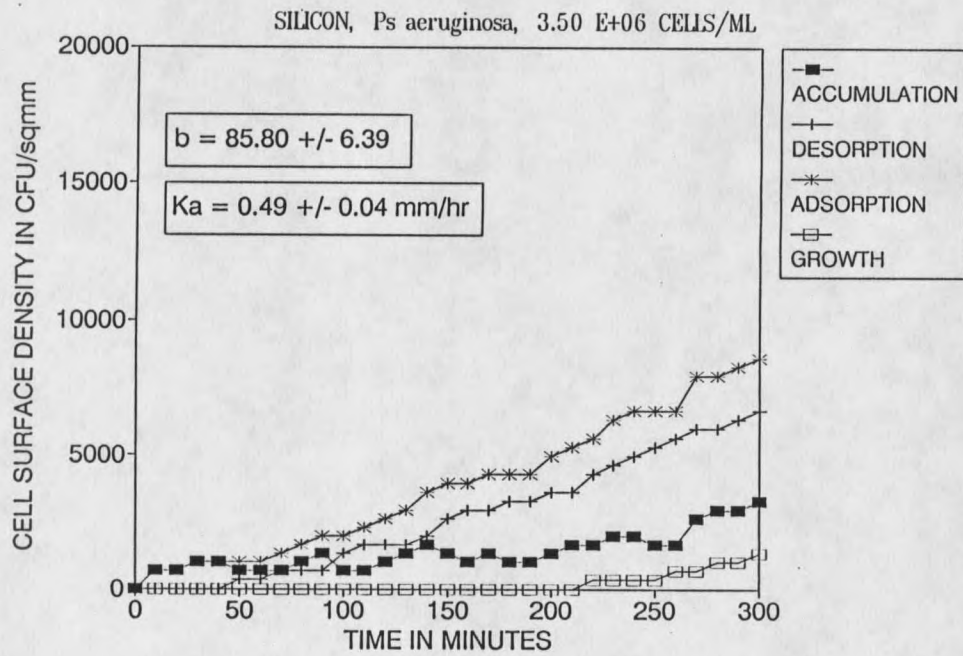


Figure 5. Cell accumulation of *Pseudomonas aeruginosa* on silicon using a bulk water concentration of 3.5×10^6 cells ml^{-1} (Figure 5 a) and a sterile nutrient (40 ppm C) after initial cell colonization of 2100 CFU mm^{-2} (Figure 5 b). Shear stress 0.75 N m^{-2} .

316-Stainless Steel

A freshly polished 316 stainless steel surface had a RMS surface roughness of 77 Å when measured in vertical direction. After this surface was exposed to air for several weeks, the RMS surface roughness increased to 120 Å (Figure 6).

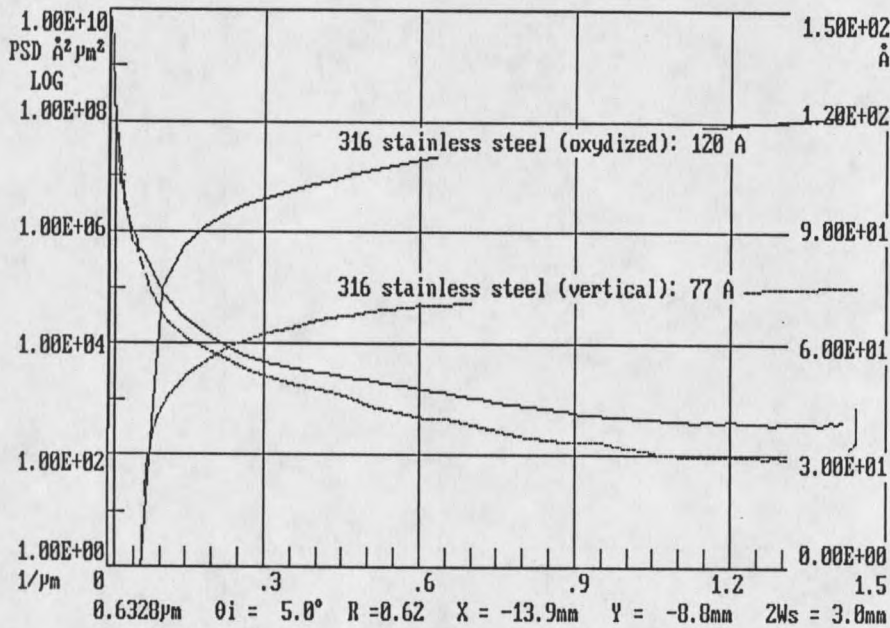


Figure 6. Results from a laser light scatter measurement on the 316 stainless steel surface. Power spectral density (PSD) is plotted versus frequency. The integration of this curves provide values for RMS surface roughness. A fresh polished surface, measured in vertical direction is compared with a highly oxidized surface, measured in vertical direction.

The bulk water concentration was constant during the accumulation experiment at 1.10×10^6 cells ml^{-1} (Figure 7 a). The adsorption velocity was $K_a = 1.82 \text{ mm hr}^{-1}$, the probability of desorption was $b = 0.30$, and the growth rate on the substratum ($K_g = 0.33 \text{ hr}^{-1}$) was higher than the rate of erosion ($K_e = 0.09 \text{ hr}^{-1}$) (Figure 7 and Table 4).

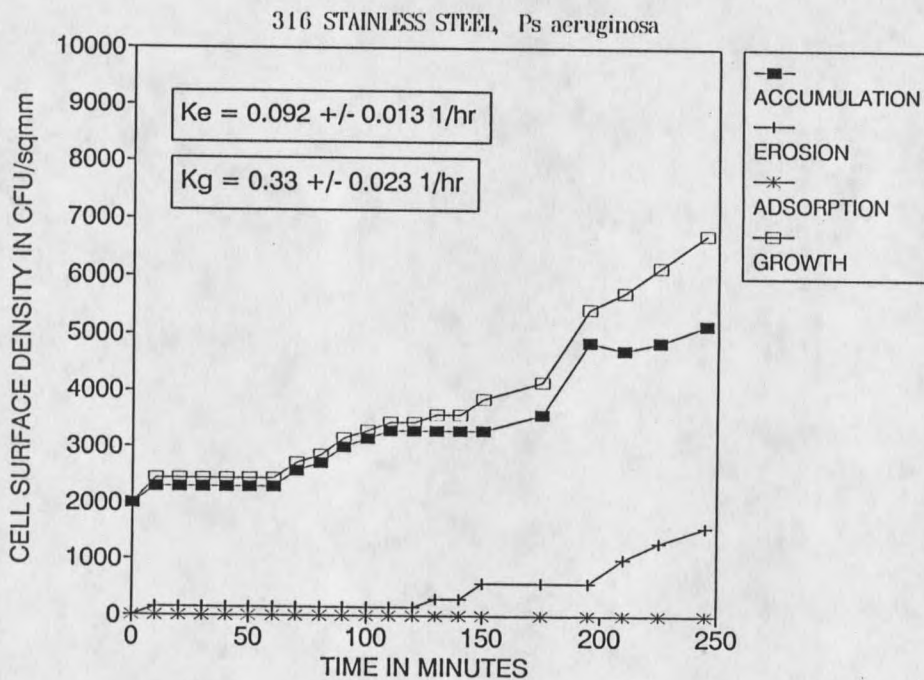
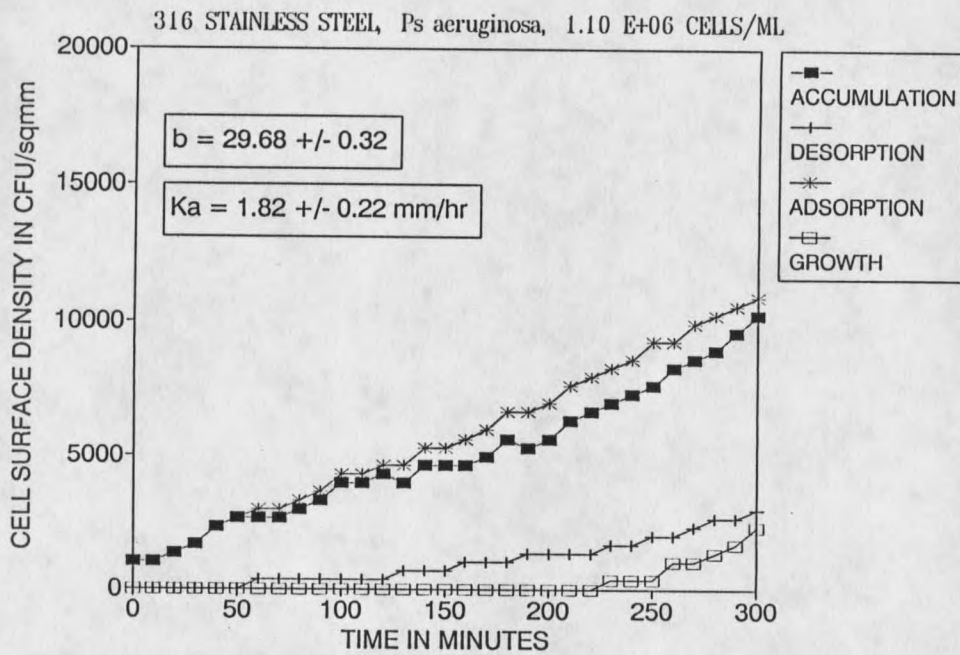


Figure 7. Cell accumulation of *Pseudomonas aeruginosa* on 316 stainless steel using a bulk water concentration of 1.1×10^6 cells ml^{-1} (Figure 7 a) and a sterile nutrient (40 ppm C) after initial cell colonization of 2000 CFU mm^{-2} (Figure 7 b). Shear stress 0.75 N m^{-2} .

Table 4. Pseudomonas aeruginosa, Summary of the Results
(shear stress 0.75 Nm^{-1})

rate constant units		copper	silicon	316 stainless	glass*
RMS	[Å]	150	27	121	-
Ka	[mm hr ⁻¹]	2.22±0.43	0.47±0.04	1.84±0.22	1.14
b	[-]	0.21±0.02	0.86±0.06	0.30±0.02	0.62±0.18
Ke	[hr ⁻¹]	-	0.32±0.01	0.09±0.01	0.32±0.08
ε	[-]	0.032±0.006	0.007±0.001	0.026±0.003	0.016
Φ	[-]	0.026±0.005	0.006±0.0004	0.022±0.002	0.018
g	[hr]	-	2.47±0.71	2.10±0.38	1.36±0.29
kg	[hr ⁻¹]	0.00	0.28±0.08	0.33±0.06	0.51±0.11

* Results from Escher (1986)

Surface Roughness

RMS surface roughness was measured for all metal surfaces used in the experiments and was correlated to adsorption velocity (Figure 8). Adsorption velocity increased with increasing roughness of the substratum and the probability of desorption decreased with increasing surface roughness. Hence, the irreversible adsorption was influenced even stronger by the roughness of the substratum.

Pseudomonas fluorescens (mot+), Results

Surface Colonization of Pseudomonas fluorescens (mot+)

Cellular colonization of Pseudomonas fluorescens (mot+) was different from the behavior of Pseudomonas aeruginosa. Pseudomonas fluorescens (mot+) cells were transported as single cells to the

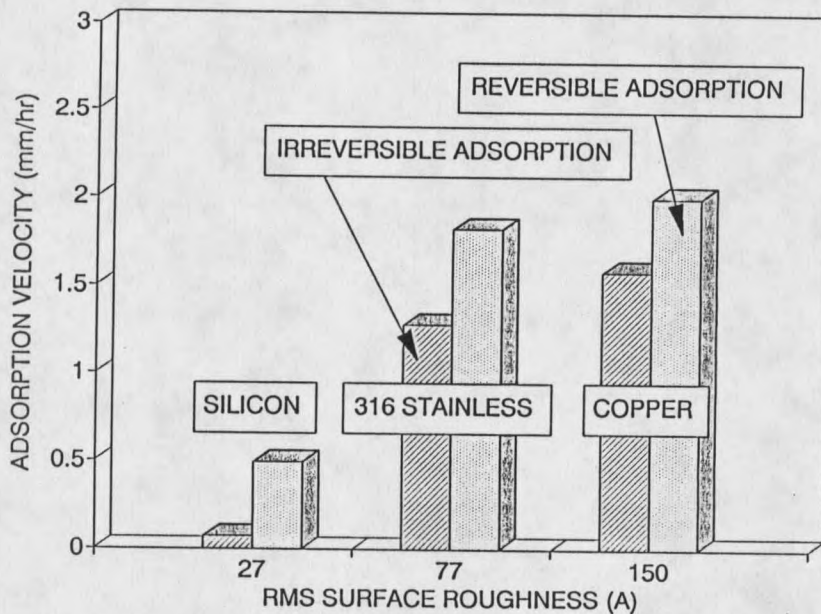


Figure 8. Adsorption velocity of *Pseudomonas aeruginosa* versus surface roughness of the substratum. Shear stress 0.75 N m^{-2} .

fluorescens (mot+) cells were transported as single cells to the substratum but adsorption occurred more often in clusters. Desorption of cells even from clusters, occurred as single cells in most cases.

Growth rate and the rate of erosion were not determined for *Pseudomonas fluorescens*.

316 Stainless Steel

Cell accumulation of *Pseudomonas fluorescens* (mot+) on 316 Stainless was observed at a cell concentration of $1.3 \times 10^6 \text{ cells ml}^{-1}$ (Figure 9). *Pseudomonas fluorescens* (mot+) had an adsorption velocity on Stainless Steel of $K_a = 0.30 \text{ mm hr}^{-1}$ and a probability of desorption $b = 0.61$. The kinetic results for adsorption and desorption of *Pseudomonas fluorescens* (mot+) on stainless steel and other substrata are summarized in Table 5.

Polycarbonate

Cell accumulation of Pseudomonas fluorescens (mot+) on polycarbonate was observed at a bulk water cell concentration of 3.85×10^6 cells ml^{-1} (Figure 10 and Table 5). The adsorption velocity on polycarbonate was $K_a = 0.23 \text{ mm hr}^{-1}$. The probability of desorption ($b = 0.03$) was relatively low on polycarbonate.

Glass

Cell accumulation of Pseudomonas fluorescens (mot+) on glass was observed at a bulk water cell concentration of 3.85×10^6 cells ml^{-1} (Figure 11 and Table 5). The adsorption velocity on glass was $K_a = 0.25 \text{ mm hr}^{-1}$, the probability of desorption was $b = 0.41$.

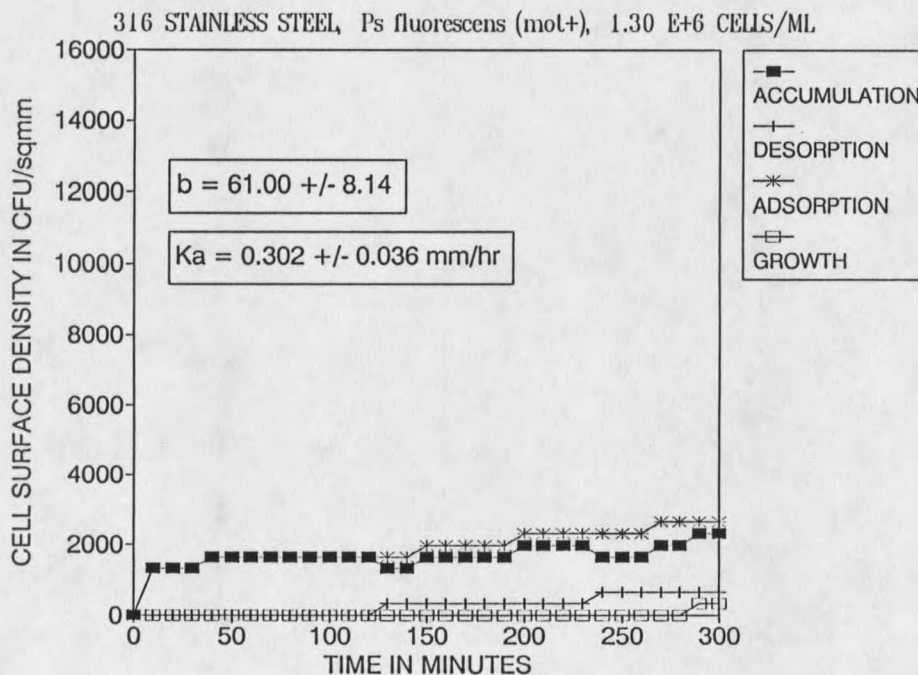


Figure 9. Cell accumulation of Pseudomonas fluorescens (mot+) on 316 stainless steel using a bulk water concentration of 1.3×10^6 cells ml^{-1} . Shear stress 0.75 N m^{-2} .

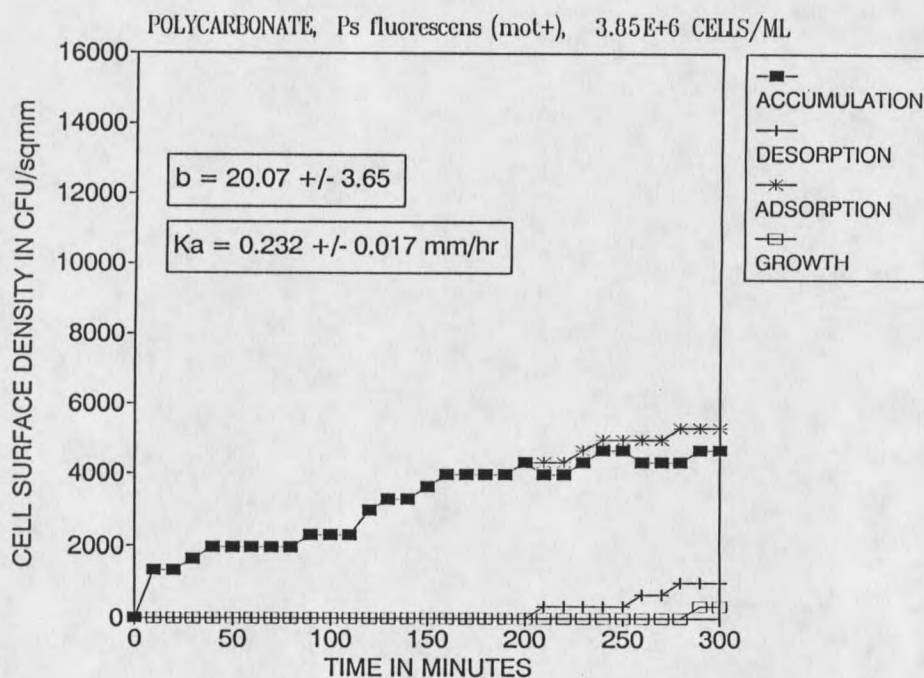


Figure 10. Cell accumulation of *Pseudomonas fluorescens* (mot+) on polycarbonate using a bulk water concentration of 3.85×10^6 cells ml^{-1} . Shear stress 0.75 N m^{-2} .

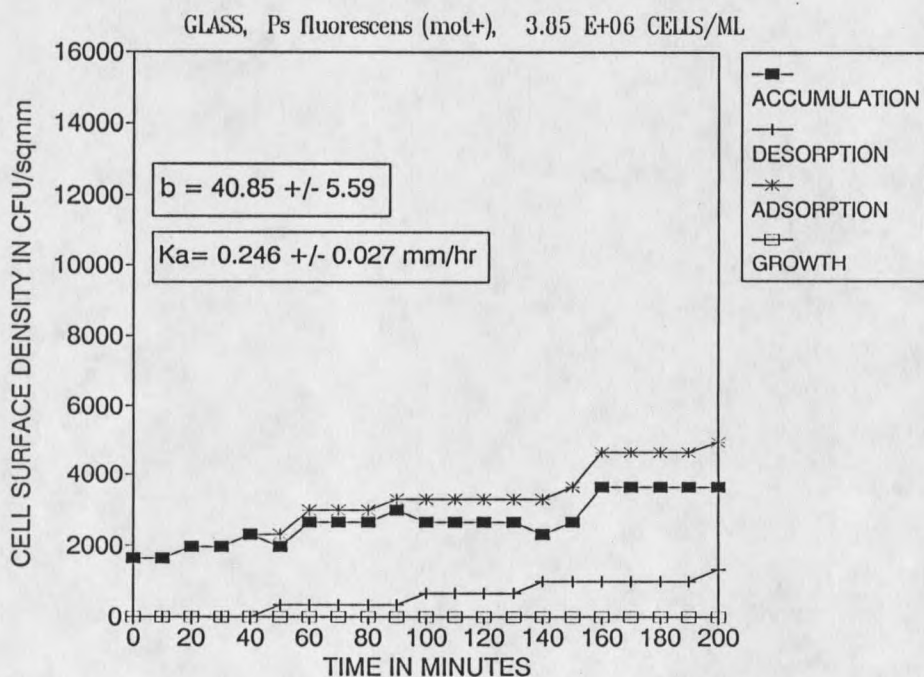


Figure 11. Cell accumulation of *Pseudomonas fluorescens* (mot+) on glass using a bulk water concentration of 3.85×10^6 cells ml^{-1} . Shear stress 0.75 N m^{-2} .

using a bulk water concentration of 3.85×10^6 cells ml^{-1} . Shear stress 0.75 N m^{-2} .

Table 5. Pseudomonas fluorescens (mot+), Summary of the Kinetic Results (shear stress 0.75 Nm^{-2}).

rate constant	Unit	316 Stainless	Polycarbonate	Glass
Ka	[mm hr ⁻¹]	0.30±0.03	0.23±0.02	0.25±0.01
b	[-]	0.61±0.20	0.20±0.22	0.41±0.25
ε	[-]	0.0042±0.0005	0.0032±0.0004	0.0034±0.0004
Φ	[-]	0.0036±0.0004	0.0028±0.0002	0.0029±0.0003

Surface Roughness

Numbers for RMS surface roughness for the transparent surfaces cannot be given, because the power spectral density theory to calculate RMS roughness for transparent surfaces does not exist. However, a laser light scatter measurement on these surfaces permitted a qualitative estimate indicating that the polycarbonate surface was slightly rougher than the glass.

Results with Pseudomonas fluorescens (mot-)

Surface Colonization of Pseudomonas fluorescens (mot-)

Surface colonization of Pseudomonas fluorescens (mot-) cells were similar to the motile parent. Cells did get transported as single cells to the substratum but adsorption occurred often in clusters. Desorption of cells even from clusters occurred as single cells in most cases.

This excluded the possibility that these cells switched back to their mot+ origin.

316 Stainless Steel

Cell accumulation of Pseudomonas fluorescens (mot-) on 316 stainless was observed at a bulk water cell concentration of 3.50×10^6 cells ml⁻¹ (Figure 12 and Table 6). The adsorption velocity of Pseudomonas fluorescens (mot-) on 316 Stainless Steel was $K_a = 0.18$ mm hr⁻¹, the probability of desorption from the metal substratum was $b = 0.84$.

Polycarbonate

Cell accumulation of Pseudomonas fluorescens (mot-) on polycarbonate was observed at a bulk water cell concentration of 5.15×10^6 cells ml⁻¹ (Figure 13 and Table 6). The adsorption velocity was $K_a = 0.15$ mm hr⁻¹ and the probability of desorption was $b = 0.03$.

Glass

Cell accumulation of motile Pseudomonas flourescens on glass was observed at a bulk water cell concentration of 8.90×10^6 cells ml⁻¹ (Figure 14 and Table 6). The adsorption velocity on glass was $K_a = 0.09$ mm hr⁻¹ and the probability of desorption was $b = 0.23$.

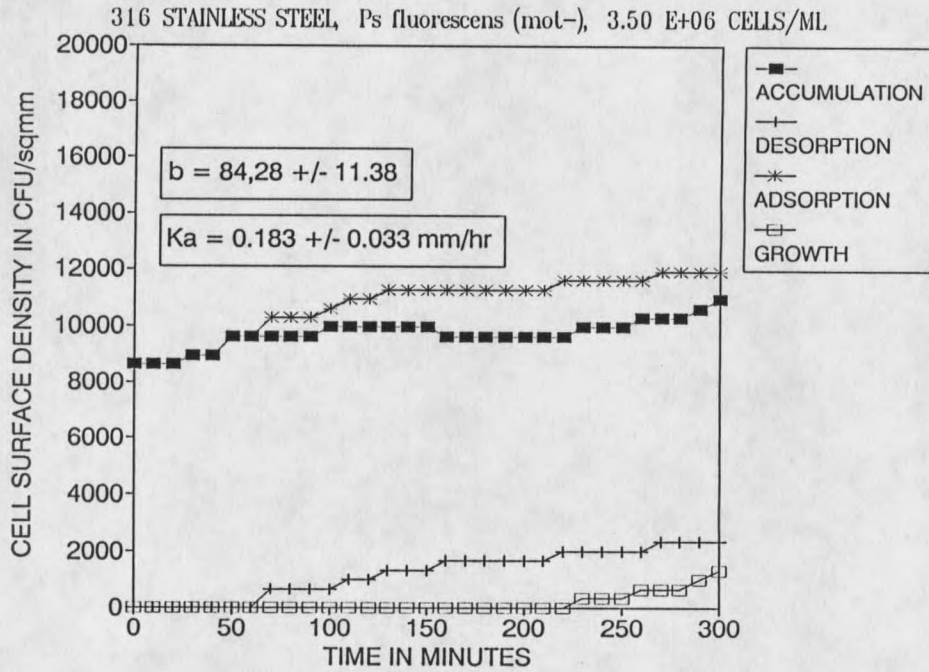


Figure 12. Cell accumulation of *Pseudomonas fluorescens* (mot-) on 316 stainless steel using a bulk water concentration of 3.5×10^6 cells ml^{-1} . Shear stress 0.75 N m^{-2} .

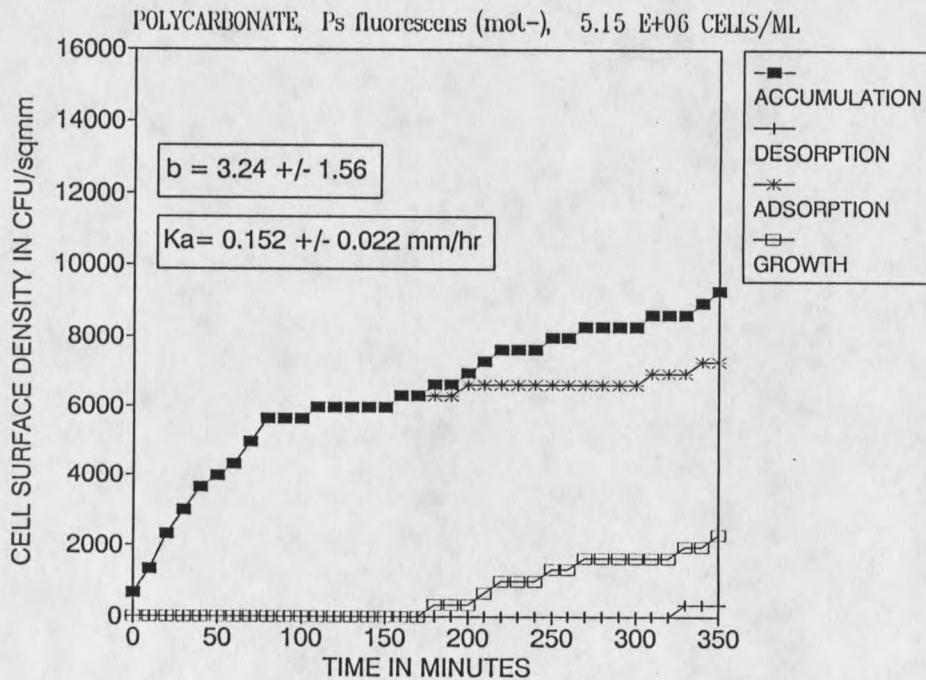


Figure 13. Cell accumulation of *Pseudomonas fluorescens* (mot-) on polycarbonate using a bulk water concentration of 5.15×10^6 cells ml^{-1} . Shear stress 0.75 N m^{-2} .

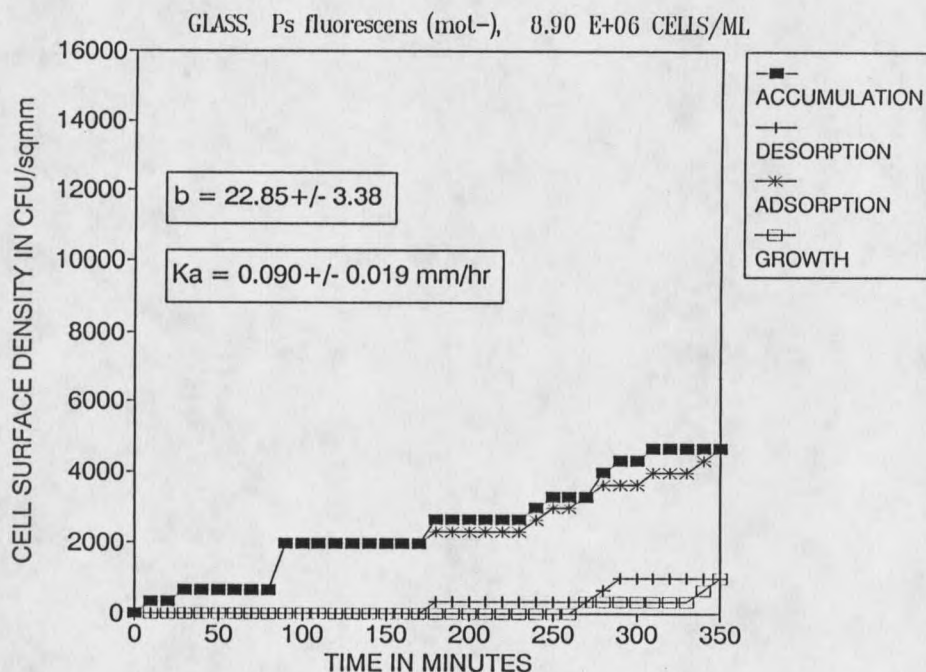


Figure 14. Cell accumulation of *Pseudomonas fluorescens* (mot-) on glass using a bulk water concentration of 8.9×10^6 cells ml^{-1} . Shear stress 0.75 N m^{-2} .

Table 6 *Pseudomonas fluorescens* (mot-), Summary of the Kinetic Results (shear stress 0.75 Nm^{-2}).

rate constant	Unit	316 Stainless	Polycarbonate	Glass
Ka	$[\text{mmhr}^{-1}]$	0.18 ± 0.04	0.15 ± 0.02	0.09 ± 0.02
b	$[-]$	0.84 ± 0.11	0.03 ± 0.01	0.23 ± 0.03
ϵ	$[-]$	14.65 ± 0.47	7.84 ± 0.18	3.14 ± 0.94
Φ	$[-]$	0.48 ± 0.03	0.33 ± 0.01	0.17 ± 0.06

Surface Colonization and Dislocations on Stainless Steel

A higher adsorption rate at cracks, interruptions or other dislocations on the surface was not observed for any bacteria species in

any of the experiments. However, all dislocations found on the mechanically polished surfaces were in the micro range ($<0.1 \mu\text{m}$ in width) and did not change hydrodynamics on the surface. A typical colonization pattern on 316 stainless steel for low cell surface densities showed a random cell distribution. Dislocations were not colonized at any higher level than other places on the surface.

Pseudomonas aeruginosa - Starvation and
Adsorption to 316 Stainless Steel

The chemostat nutrient supply was cut off after steady state conditions were reached to study cellular colonization of Pseudomonas aeruginosa in oligotrophic environments. Thus, the former chemostat was changed into a batch reactor. Aeration and agitation were still maintained. The cell size distribution and the cell concentration were monitored over time. Adsorption/desorption of starved cells were observed at various durations of starvation. At defined intervals, the diluted effluent was pumped over the 316 stainless steel surface at a constant shear stress of 0.75 N m^{-2} . The cell concentration was constant during one adsorption experiment with values between 10^6 and 10^7 cells ml^{-1} . The cellular accumulation curves are presented in the Appendix. Contamination was observed after 900 hours of starvation and the experiment was terminated after 1224 hours. The viable plate counts after 816 hours of starvation showed no contamination (Figure 15).

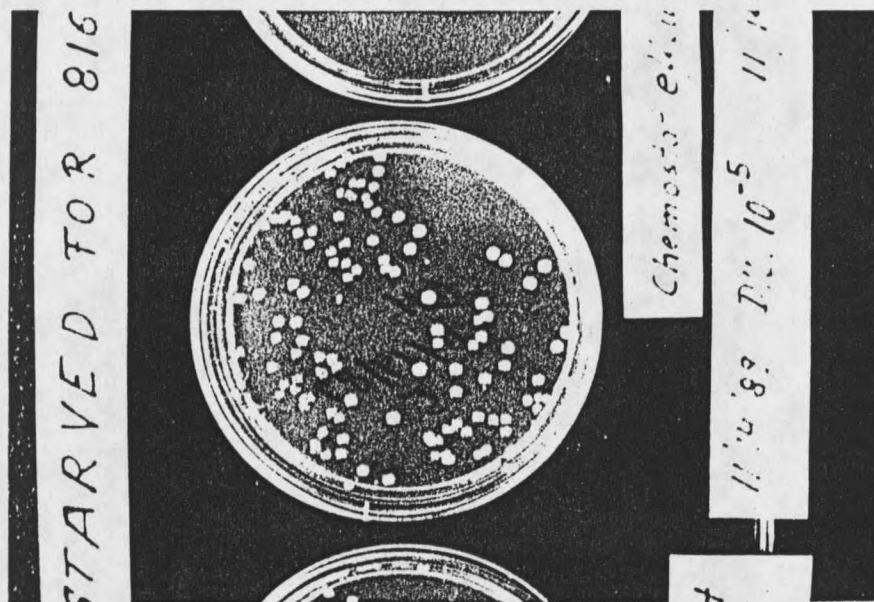


Figure 15. Photograph, plate count on R2A medium of Pseudomonas aeruginosa starved for 816 hours.

Dwarfing and Fragmentation

Immediate responses of Pseudomonas aeruginosa to starvation were size reduction (dwarfing) and an increase in cell concentration (fragmentation). Total and viable cell concentrations increased after 24 hours followed by a period of constant cell concentration until 200 hours of starvation (Figure 16). From 200 to 300 hours duration of starvation, the cell concentration decreased rapidly. After 300 hours of starvation the rate of decrease slowed. The average size distribution of Pseudomonas aeruginosa was determined as cell surface area as a function of duration of starvation (Figure 17). The average size of healthy cells was determined at $0.91 \mu\text{m}^2$. After 24 hours of starvation, the average size decreased to $0.58 \mu\text{m}^2$. For longer durations of starvation the average size stayed relatively constant between 0.45 and $0.58 \mu\text{m}^2$.

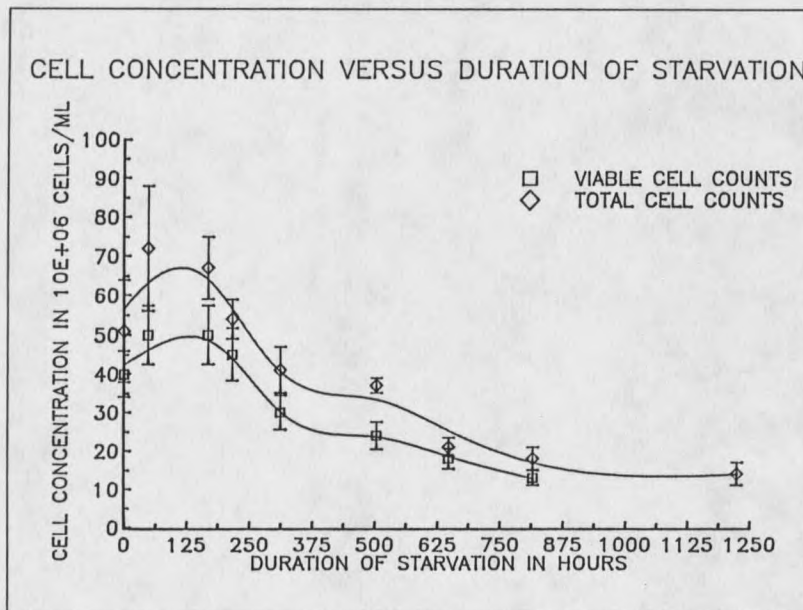


Figure 16. Total and viable suspended cell concentration versus duration of starvation, (curve fit with Axum software).

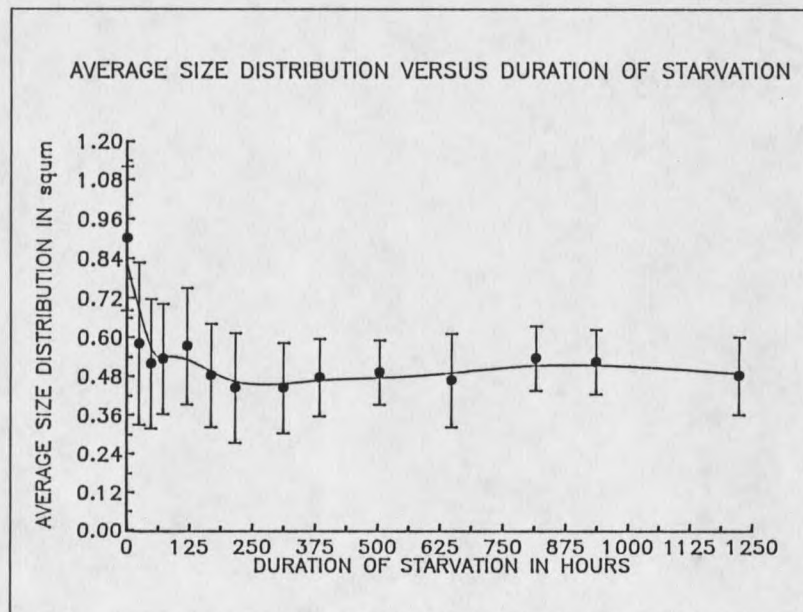


Figure 17. Cell size distribution (mean and standard deviation) of *Pseudomonas aeruginosa* versus duration of starvation, (curve fit with Axum software).

Surface Colonization of Starved Pseudomonas aeruginosa on 316 Stainless Steel

For Pseudomonas aeruginosa on 316 Stainless Steel adsorption velocity was a function of duration of starvation (Figure 18). Adsorption velocity was determined from linear regression analysis of a 100 minutes cellular accumulation experiment (Appendix, Figure 28-39). The adsorption velocity (K_a) was calculated using the viable cell counts (K_{a_v}) as well as the total cell counts (K_{a_t}). Because viable counts were consistently lower than total counts the adsorption velocity was higher when using viable counts. In either case, the adsorption velocity decreased for durations of starvation up to 500 hours in a linear fashion. Past 500 hours starvation, adsorption velocity remained at a relatively constant level. Values for K_{a_t} and K_{a_v} were $0.10-0.35 \text{ mm hr}^{-1}$ and $0.4-0.6 \text{ mm hr}^{-1}$, respectively. The values of K_{a_t} and K_{a_v} for healthy cells ($\mu = 0.2 \text{ hr}^{-1}$) were measured at 1.25 and 1.56 mm hr^{-1} , respectively.

The probability of desorption (b) from the stainless steel surface decreased during the first 300 hours of starvation and remained at its lowest values through 800 hours (Figure 19). The probability of desorption increased slightly with longer durations of starvation and remained at a relatively constant value of $b = 0.07$.

In all starvation experiments, no growth or cell division was seen on the substratum during the time period measured .

Cellular Motility

The K_a values were chosen to present the adsorption data because cellular motility is not required for its calculation. Cellular motility

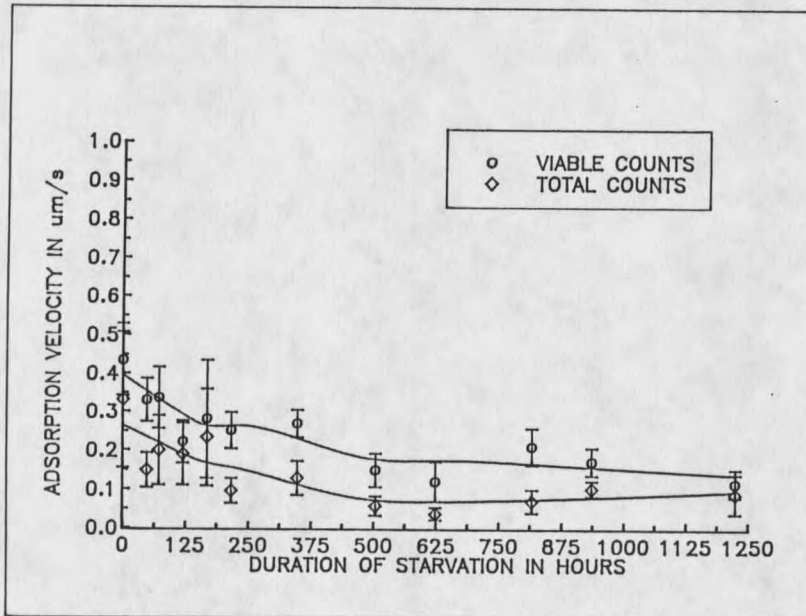


Figure 18. Adsorption velocity of *Pseudomonas aeruginosa* on 316 stainless steel at different stages of starvation. Adsorption velocity was determined using the total number of cells as well as using the viable cell concentration in the bulk water, (curve fit with Axum software).

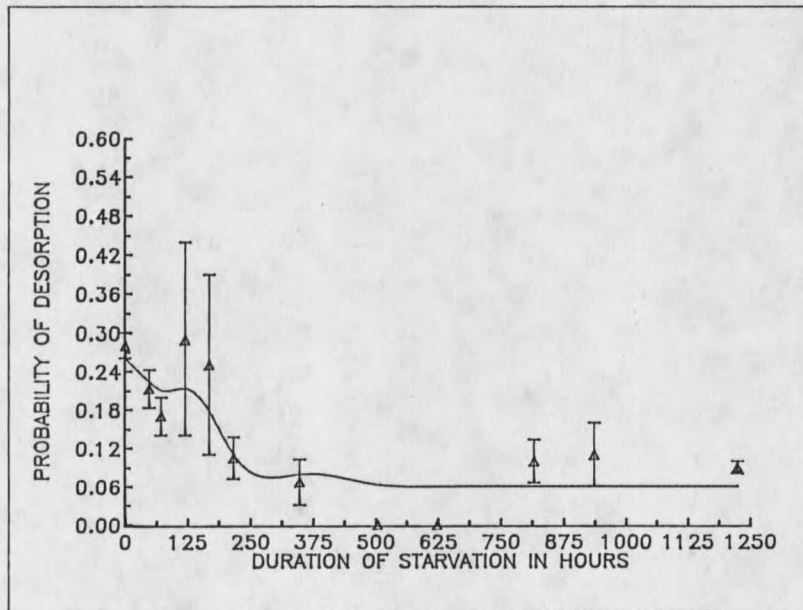


Figure 19. Probability of desorption for adsorbed *Pseudomonas aeruginosa* at different stages of starvation at a 316 stainless steel substratum, (curve fit with Axum software).

during starvation was qualitatively determined after 816 hours duration of starvation. The average random free runs were observed at $33 \pm 11 \mu\text{m}$ from 47 observations. For the cellular swimming speed only a rough estimate can be given with $v_r = 100$ to $200 \mu\text{m s}^{-1}$.

SIMULATION OF CELL ACCUMULATION

Cellular colonization on 316 stainless steel, copper, and silicon could be simulated for Pseudomonas aeruginosa from experimental results (Equation 12). From the results with Pseudomonas fluorescens, the two species could be used for comparison of early surface colonization. The growth rate on the substratum was calculated for low nutrient conditions (Equation 9), whereas the value for the maximum growth rate at 22 °C was determined experimentally for Pseudomonas aeruginosa. For Pseudomonas fluorescens the value of the maximum growth rate on glass was used determined by Korber et. al. (1989). Certain parameters were varied individually, and cellular accumulation was simulated.

Bulk Water Cell Concentration

The stainless steel surface coverage for a bulk water cell concentration of 10^6 cells ml^{-1} after 700 minutes was predicted to be 10 % of the total surface area (Figure 20). For a cell concentration of $4 \cdot 10^6$ the cell covered surface area was simulated to be 33 %.

Fluid Shear Stress

Cell accumulation of Pseudomonas aeruginosa is simulated on 316 stainless steel at various fluid shear stresses on the substratum (Figure 21). With an exponential influence of shear stress to adsorption (Escher, 1986), cellular accumulation decreased with higher shear on the surface.

Substrata and Bulk

Water Nutrient Concentration

Cell accumulation of Pseudomonas aeruginosa is presented for three reflective substrata (Figure 22). Cell concentration was assumed constant at 2×10^6 cell ml^{-1} in the bulk water and nutrient was assumed to be not limiting. The adsorbed bacteria grow at their maximum rate found on each surface. The Silicon surface showed a total area coverage (TAC) of less than 1% after 700 minutes, Copper had a TAC value of 3.4 % and 316 stainless steel showed the highest TAC value of 16 % after 700 minutes. A similar simulation of cell accumulation of Pseudomonas aeruginosa on 316 stainless steel, copper and silicon was performed for a low nutrient environment (Figure 23). The total coverage on the silicon surface than was still approximately 1 %. The TAC on copper also did not change because there was no growth on the copper surface. The TAC on the stainless steel surface as a result of the slower growth process decreased to 5 %.

Mixed Population

Cell accumulation of a mixed population of Pseudomonas aeruginosa and Pseudomonas fluorescens (mot+) and Pseudomonas fluorescens (mot-) is presented in Figure 24. Growth rate for both species were identical and there were no toxic or other chemical interactions between the two species assumed. The simulation was proceeded until TAC was 100 %. The fraction of total area covered by Pseudomonas aeruginosa was 94 %, the fraction of area covered by Pseudomonas fluorescens (mot+) was 5 % and the fraction of area covered by Pseudomonas fluorescens (mot-) was about 1 %.

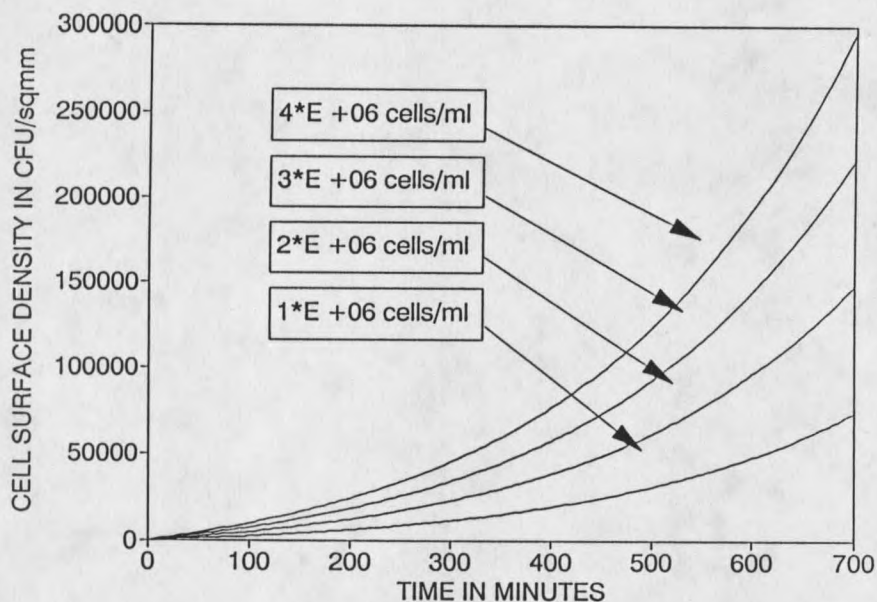


Figure 20. Simulation of cell accumulation of *Pseudomonas aeruginosa* on 316 stainless steel at various bulk water cell concentrations. Shear stress 0.75 N m^{-2} .

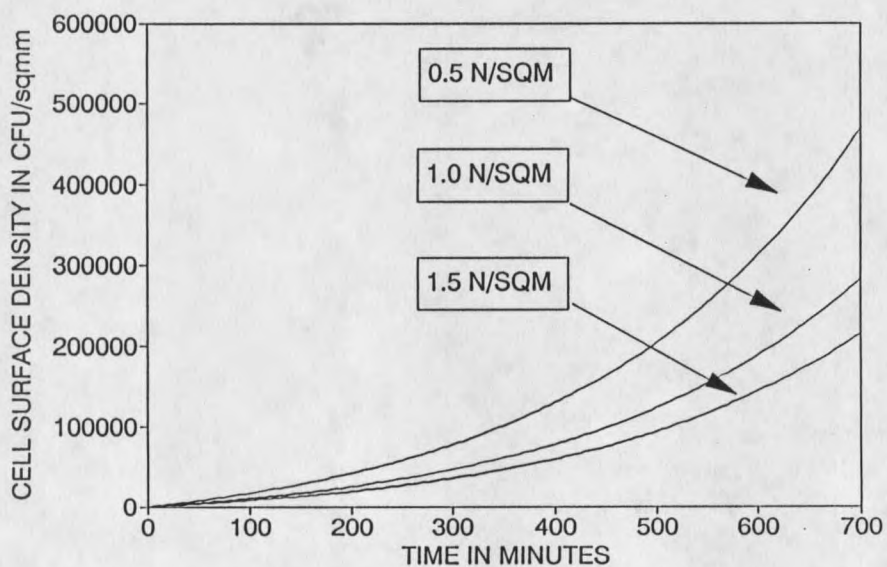


Figure 21. Simulation of cell accumulation of *Pseudomonas aeruginosa* on 316 stainless steel at various shear stress. Bulk water cell concentration $6 \cdot 10^6 \text{ cells ml}^{-1}$.

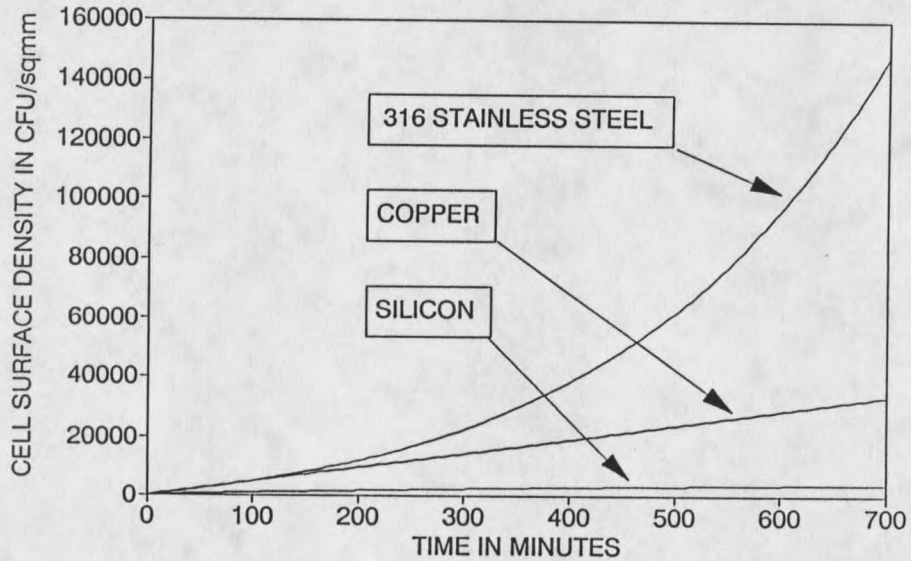


Figure 22. Simulation of cell accumulation of *Pseudomonas aeruginosa* on 316 stainless steel, copper, and silicon at rich nutrient conditions in the bulk water ($S > 10$ ppm C). Bulk water cell concentration 2×10^6 cells ml^{-1} and shear stress 0.75 N m^{-2} .

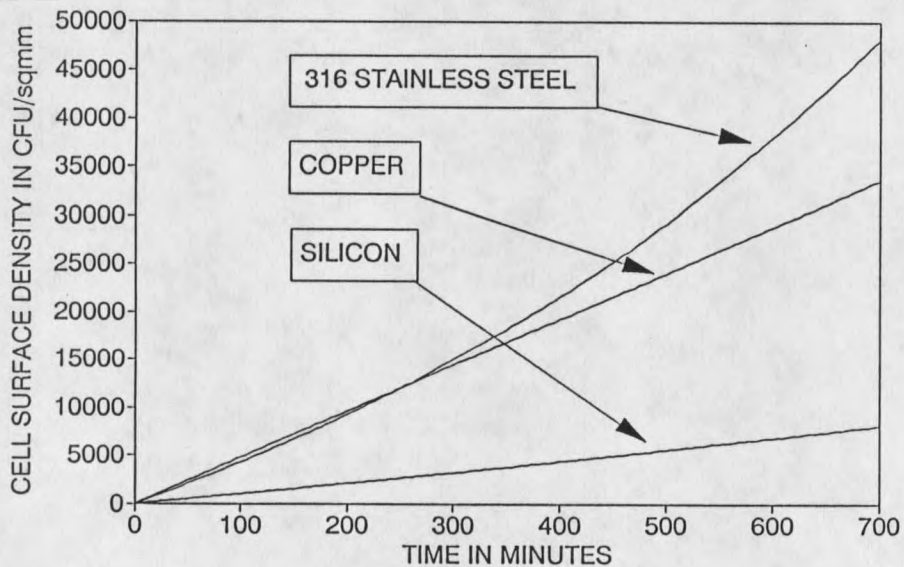


Figure 23. Simulation of cell accumulation of *Pseudomonas aeruginosa* on 316 stainless steel, copper, and silicon at low nutrient conditions in the bulk water ($S = 0.6$ ppm C). Bulk water cell concentration 2×10^6 cells ml^{-1} and shear stress 0.75 N m^{-2} .

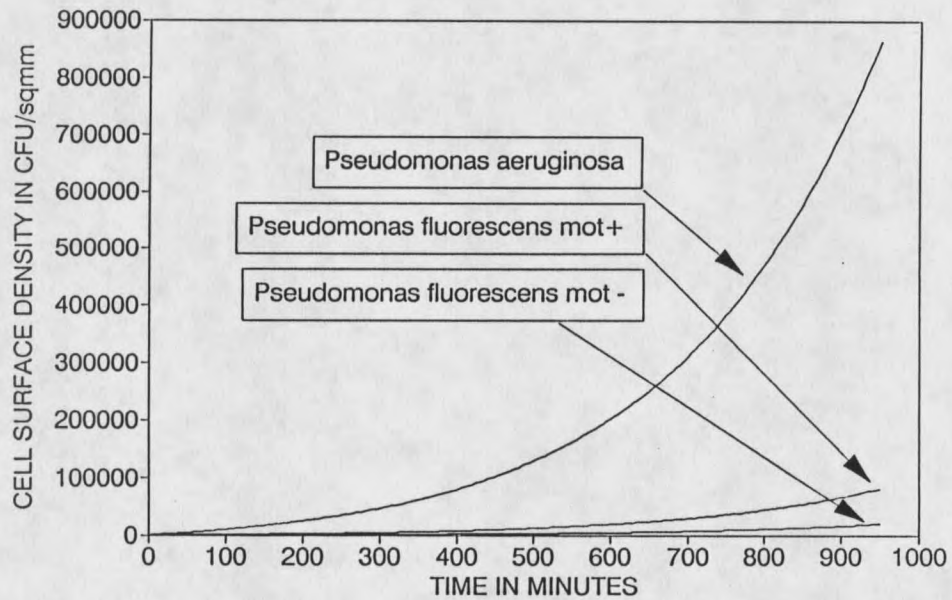


Figure 24. Simulation of cell accumulation of a mixed population of *Pseudomonas aeruginosa*, *Pseudomonas fluorescens* (mot+), and *Pseudomonas fluorescens* (mot-) on 316 stainless steel. Cell concentration $4 \cdot 10^6$ cells ml^{-1} and shear stress 0.75 N m^{-2} .

DISCUSSION

Comparison of *Pseudomonas aeruginosa* on Various Substrata

In all experiments, adsorption rate and desorption rate were found to be independent of the accumulated cell surface density and were treated as first order with respect to bulk water cell concentration. The rate of erosion and replication was found to be independent of the bulk water cell concentration and first order with respect to the accumulated cell surface density. This finding is consistent with the results obtained by Escher (1986).

Reversible and irreversible adsorption velocity of *Pseudomonas aeruginosa* were dependent on the substratum (Figure 25). The lowest rates of reversible and irreversible adsorption were found on the very smooth monocrystalline silicon surface. The irreversible adsorption velocity was calculated at 0.07 mm hr^{-1} . Only 14 % of all reversibly adsorbed cells became irreversibly adsorbed. The silicon surface also had the lowest RMS surface roughness value of 25 Å. 316 stainless steel had an RMS surface roughness value of 77 Å and an irreversible adsorption velocity of 1.33 mm hr^{-1} which was 20 times higher than on silicon. 70 % of all reversibly adsorbed cells became irreversibly adsorbed over time on the stainless steel surface. Copper was the roughest surface investigated with an average RMS roughness value of 150 Å and an irreversible adsorption velocity of 1.58 mm hr^{-1} which was 23 times higher than on silicon. 79 % of all reversibly adsorbed cells became irreversibly adsorbed over time on copper. Hence, surface roughness strongly influenced bacterial

accumulation on a substratum without regard to the material. Vanhaecke et al. reported an stronger influence of surface roughness for less hydrophobic cells but, overall a positive curvelinear correlation between surface roughness of stainless steel and the rate of adsorption of *Pseudomonas aeruginosa*. Surface hydrophobicity of the substratum and surface roughness are directly related. Therefore, a high surface hydrophobicity could exaggerate the effect of high surface roughness on cell accumulation at solid-water interfaces. A low surface hydrophobicity on the other hand could depress the effect of high surface roughness on bacterial adsorption.

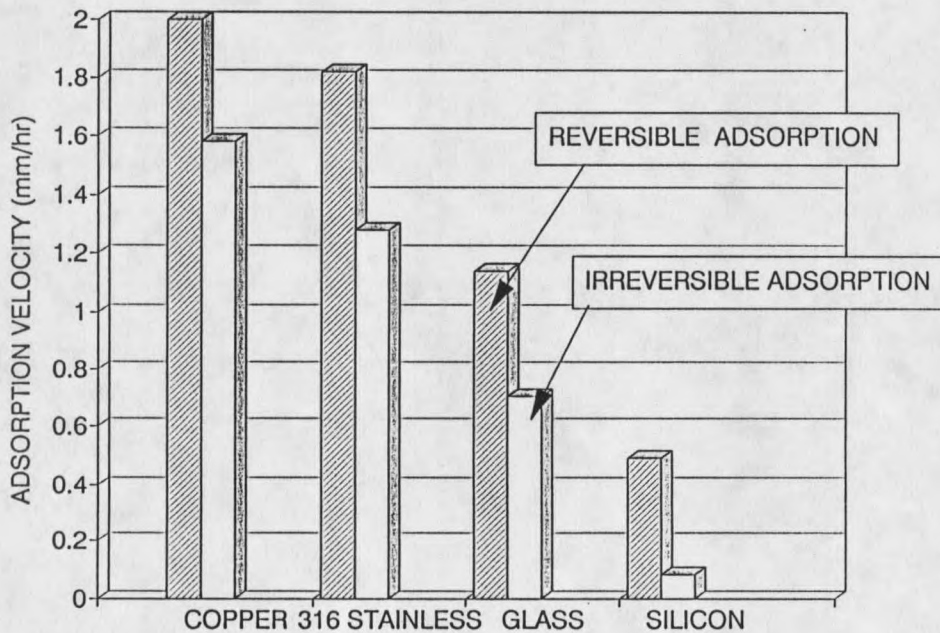


Figure 25. Comparison of reversible and irreversible adsorption velocity of *Pseudomonas aeruginosa* on various substrata. Shear stress 0.75.

There was no cell replication of Pseudomonas aeruginosa on copper (Figure 4), which indicates that the adsorbed cells were metabolically inactive, dead or severely inhibited. With sufficient exposure time, a cell monolayer accumulated on the copper substratum and replication of cells in the upper bacteria layers were observed. The greater the distance of the cells from the copper surface and, consequently, a lower concentration of copper ions in the cell microenvironment (concentration gradient) may have reduced the inhibitory effect. The reduced toxicity of copper ions could also be a result of copper complexation by the extracellular polymer in the biofilm. In any case, biofilms provide a protection for the cells from the toxic effects of copper.

The rate of replication was found to be lower for cells adsorbed to the monocrystalline silicon or stainless steel surface than for cells adsorbed to glass. The generation time was 2.1 hours ($K_g = 0.33 \text{ hr}^{-1}$) on the stainless steel surface and 2.5 hours ($K_g = 0.28 \text{ hr}^{-1}$) on silicon. Escher (1986) found a generation time for Pseudomonas aeruginosa on a smooth glass substratum of 1.36 hours ($K_g = 0.551 \text{ hr}^{-1}$) and a shear stress dependent separation rate of 0.067 hr^{-1} . The growth rates on all investigated surfaces but copper were found to be higher than the growth rate in the chemostat ($\mu = 0.2 \text{ hr}^{-1}$) but lower than the maximum growth rate of Pseudomonas aeruginosa ($\mu_{\text{max}} = 0.45 \text{ hr}^{-1}$). The reason for the higher growth rate on the silicon and 316 stainless steel substrata than in the chemostat could be that the substrate concentration in the flow cell bulk water (40 gm^{-3}) was higher than the substrate concentration in the chemostat (5 gm^{-3}). The growth rates for adsorbed cells were below the maximum growth rate for planktonic cells and the lower temperature at the

solid-water interface (20-24°C) may have been a contributing cause. Also, the energy expended in initial adsorption of a cell to the metal should not be neglected. The energy of adsorption could explain the slower growth on the smoother silicon surface where the cell adsorption strength was lower than on rougher surfaces. On 316 stainless steel, growth may be inhibited by nickel and chromium ions which diffuse through the metal oxide layer. 316 stainless steel contains nickel and chromium in a large amount (approximately 20 and 3 %, respectively). However, diffusion of these toxic metal ions must occur at a lower rate on stainless steel than on copper. The thickness of the metal oxide layer was not determined, but the oxide layer on 316 stainless steel was found to be much more homogeneous than the metal oxide layer on copper by surface roughness measurements of the oxidized surfaces (RMS surface roughness of 120 Å and 1680 Å, respectively). Hence, the composition and thickness of the metal oxide layer provide the diffusion, barrier limiting, cell growth on metallic substrata.

For most of the investigated materials the adsorption velocity had a slightly higher value during the first hour of exposure. There may be preferred sites on the surface where cells adsorbed faster. After most of these sites are occupied, adsorption becomes more energy intensive for the cells, hence the rate of adsorption was lower. Why specific sites were preferred to others cannot be answered from these experiments.

Dislocations smaller than 0.1 μm on the polished surfaces did not influence the rate of adsorption as determined by visual observation. The general surface roughness, however, exerted a large influence on adsorption and desorption.

Surface colonization on the test substrata can be simulated with the rate coefficients (Table 4). Adsorption and desorption control the rate of accumulation in the very early stages of surface colonization (linear cell accumulation over time), but become less important over time. Subsequently, growth and erosion become the rate determining processes (exponential cell accumulation over time). Growth and erosion are both first order rates with respect to cell surface density, whereas adsorption and desorption are zero order with respect to cell surface density and first order with respect to bulk liquid cell concentration. With a constant cell concentration in the bulk water the Cell surface density increases linear for the first 200 minutes. For longer time periods cumulative growth and erosion of cells lead to exponential increase and dominate the accumulation of cells at the surface.

The simulation of early surface colonization for various nutrient conditions can be simulated with the Monod equation (Equation 9). Escher's model contributes the effect of shear stress. The simulation model was tested for accuracy on 316 stainless steel and resulted in a 14 % faster total surface colonization than observed experimentally. The differences may be explained by the heterogeneous cellular colonization observed as compared to the homogeneous colonization as assumed in the model. Escher (1986) hypothesized that Pseudomonas aeruginosa produce a "protected field" around themselves, blocking further adsorption in the vicinity. This would slow the process of adsorption at high cell surface densities and a less homogeneous colonization pattern results.

Comparison of *Pseudomonas aeruginosa*
and *Pseudomonas fluorescens* (mot+)

Cellular accumulation of *Pseudomonas aeruginosa* and *Pseudomonas fluorescens* was compared on two different substrata: 316 stainless steel and glass. The results for *Pseudomonas aeruginosa* on glass were from Escher (1986) (Figure 26). Sticking efficiency, particle capture factor, and adsorption rate were dependent on the substrata in a similar manner for both species. On both substrata, adsorption was approximately 5 times slower for *Pseudomonas fluorescens* than for *Pseudomonas aeruginosa*. Consequently the sticking efficiencies for *Pseudomonas fluorescens* showed an 84 % lower value on the stainless steel surface and an 79 % lower value on the glass surface than the values obtained for *Pseudomonas aeruginosa*. The probability of desorption was slightly higher for *Pseudomonas fluorescens* on stainless steel but lower on glass. Hence cellular accumulation of *Pseudomonas fluorescens* was a much slower process than for *Pseudomonas aeruginosa*.

Pseudomonas aeruginosa is highly hydrophobic, whereas *Pseudomonas fluorescens* had an intermediate cell surface hydrophobicity (Table 3 and Figure 27). Therefore the cells with the higher cell surface hydrophobicity resulted in a higher adsorption velocity on the tested substrata. To draw a general conclusion, however, more strains with different cell surface hydrophobicity values should be tested. Vanhaecke et al. (1989) measured cell surface hydrophobicity and rate of adsorption of 15 *Pseudomonas aeruginosa* strains to stainless steel in a stagnant system and found higher number of adsorbing cells within 30 minutes

